0830-L-02 NAS1.29/3-2:00-10

NASA Tech Briefs

National Aeronautics and Space Administration

Electronic Components and Circuits

Electronic Systems

Physical Sciences

Materials

Computer Programs

Mechanics

Machinery

Fabrication Technology

Ann 20020041139

Mathematics and Information Sciences

Life Sciences

INTRODUCTION

Tech Briefs are short announcements of innovations originating from research and development activities of the National Aeronautics and Space Administration. They emphasize information considered likely to be transferable across industrial, regional, or disciplinary lines and are issued to encourage commercial application.

Availability of NASA Tech Briefs and TSPs

Requests for individual Tech Briefs or for Technical Support Packages (TSPs) announced herein should be addressed to

National Technology Transfer Center
Telephone No. **(800) 678-6882** or via World Wide Web at **www2.nttc.edu/leads/**

Please reference the control numbers appearing at the end of each Tech Brief. Information on NASA's Commercial Technology Team, its documents, and services is also available at the same facility or on the World Wide Web at **www.nctn.hq.nasa.gov**.

Commercial Technology Offices and Patent Counsels are located at NASA field centers to provide technology-transfer access to industrial users. Inquiries can be made by contacting NASA field centers and program offices listed below.

NASA Field Centers and Program Offices

Ames Research Center
Carolina Blake
(650) 604-1754 or
cblake@mail.arc.nasa.gov

Dryden Flight Research Center
Jenny Baer-Riedhart
(661) 276-3689 or
jenny.baer-riedhart@dfrc.nasa.gov

Goddard Space Flight Center
George Alcorn
(301) 286-5810 or
galcorn@gsfc.nasa.gov

Jet Propulsion Laboratory
Merle McKenzie
(818) 354-2577 or
merle.mckenzie@jpl.nasa.gov

Johnson Space Center
Hank Davis
(281) 483-0474 or
henry.l.davis1@jsc.nasa.gov

John F. Kennedy Space Center
Jim Aliberti
(321) 867-6224 or
Jim.Aliberti-1@ksc.nasa.gov

Langley Research Center
Sam Morello
(757) 864-6005 or
s.a.morello@larc.nasa.gov

Glenn Research Center
Larry Viterna
(216) 433-3484 or
cto@grc.nasa.gov

George C. Marshall Space Flight Center
Sally Little
(256) 544-4266 or
sally.little@msfc.nasa.gov

John C. Stennis Space Center
Kirk Sharp
(228) 688-1929 or
technology@ssc.nasa.gov

NASA Program Offices
At NASA Headquarters there are seven major program offices that develop and oversee technology projects of potential interest to industry:

Carl Ray
Small Business Innovation Research Program (SBIR) & Small Business Technology Transfer Program (STTR)
(202) 358-4652 or
cray@mail.hq.nasa.gov

Dr. Robert Norwood
Office of Commercial Technology (Code RW)
(202) 358-2320 or
rnorwood@mail.hq.nasa.gov

John Mankins
Office of Space Flight (Code MP)
(202) 358-4659 or
jmankins@mail.hq.nasa.gov

Terry Hertz
Office of Aero-Space Technology (Code RS)
(202) 358-4636 or
thertz@mail.hq.nasa.gov

Glen Mucklow
Office of Space Sciences (Code SM)
(202) 358-2235 or
gmucklow@mail.hq.nasa.gov

Roger Crouch
Office of Microgravity Science Applications (Code U)
(202) 358-0689 or
rcrouch@hq.nasa.gov

Granville Paules
Office of Mission to Planet Earth (Code Y)
(202) 358-0706 or
gpaules@mtpe.hq.nasa.gov

NASA TechBriefs

National Aeronautics and Space Administration

October 2000
00-10

5 Electronic Components and Circuits

9 Electronic Systems

15 Physical Sciences

21 Materials

27 Computer Programs

31 Mechanics

39 Machinery

43 Fabrication Technology

47 Mathematics and Information Sciences

This document was prepared under the sponsorship of the National Aeronautics and Space Administration. Neither the United States Government nor any person acting on behalf of the United States Government assumes any liability resulting from the use of the information contained in this document, or warrants that such use will be free from privately owned rights.

BLANK PAGE

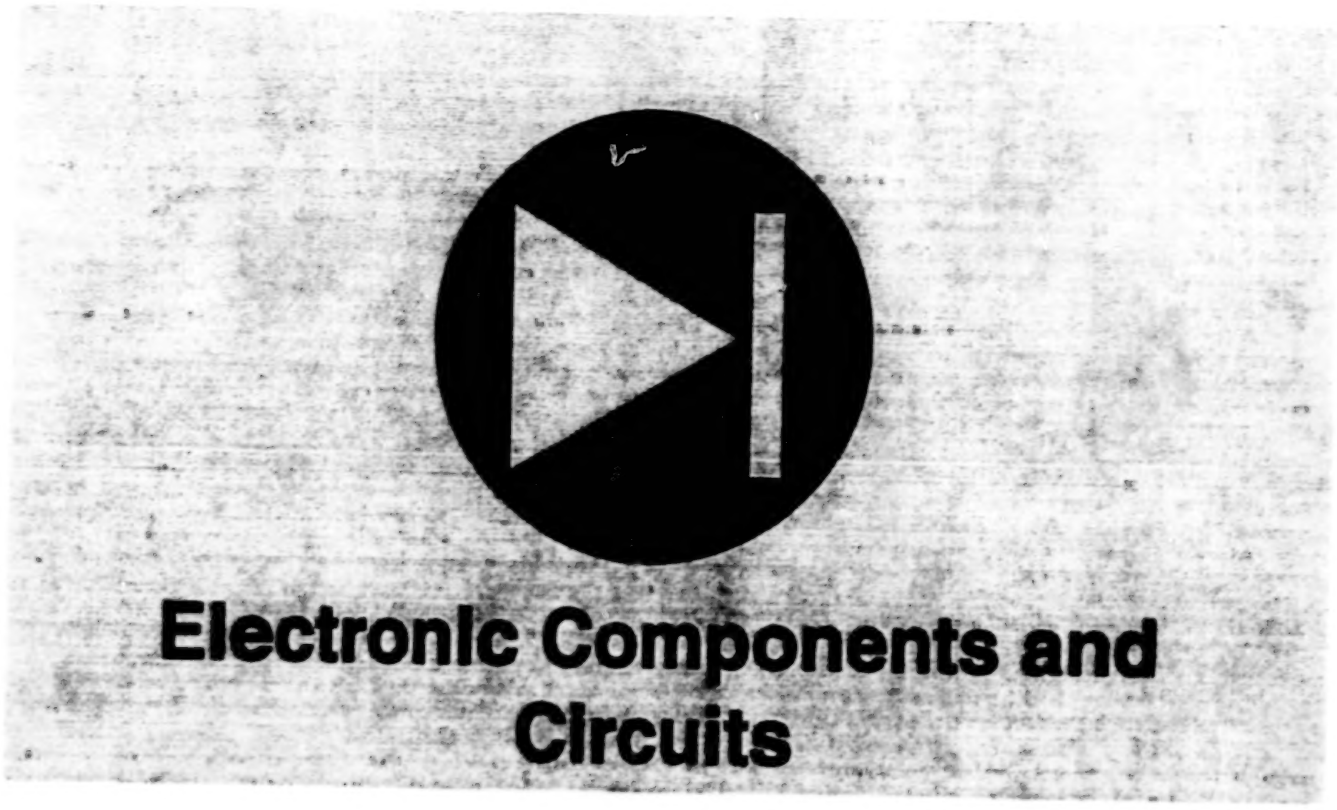

Electronic Components and Circuits

Hardware, Techniques, and Processes

7 Highly Efficient Thermoelectric Unicouples
7 Microelectromechanical SPDT Switches

BLANK PAGE

Highly Efficient Thermoelectric Unicouples

Thermal-to-electric conversion efficiencies as large as 15 percent have been predicted.

NASA's Jet Propulsion Laboratory, Pasadena, California

Advanced unicouples that contain carefully tailored combinations of thermoelectric materials are being investigated in an effort to develop thermoelectric power generators that would operate with relatively high energy-conversion efficiencies between heat-source temperatures of about 1,000 K and heat-sink temperatures of about 300 K. [A thermoelectric unicouple is a part of a thermoelectric generator; a unicouple comprises one electron-conduction (n-type) leg and one hole-conduction (p-type) leg thermally connected in parallel and electrically connected in series.] Thermoelectric generators have no moving parts, are reliable, can operate unattended in hostile environments, and are environmentally benign; because of these characteristics, they are particularly attractive for extracting electric power from waste heat from such diverse sources as geothermal power plants, industrial heat-generating processes, and automobile exhausts.

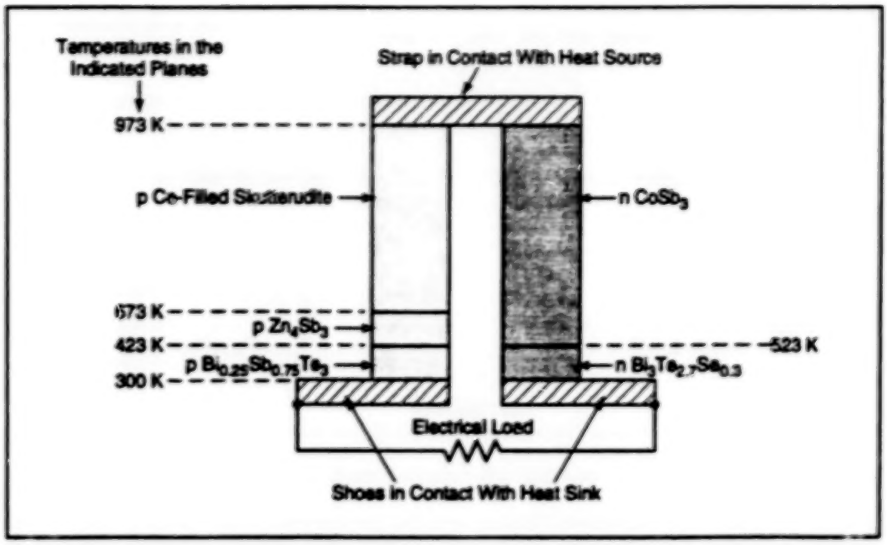

An Advanced Thermoelectric Unicouple is made of high-performance p- and n-type materials, each positioned and dimensioned so that it is exposed to a temperature interval in which its thermoelectric performance is maximized. The relative lengths of the segments shown here to scale are chosen to obtain a predicted overall thermal-to-electrical energy-conversion efficiency of about 15 percent. Fabrication and testing of the predicted prototype unicouple is in progress.

To achieve high thermal-to-electric energy-conversion efficiencies, it is desirable to operate thermoelectric devices over large temperature gradients and to maximize the performances of the thermoelectric materials in the devices. However, no single thermoelectric material is suitable for maximizing the efficiency over the entire range between the contemplated source and sink temperatures. Therefore, the approach taken in designing the present advanced thermoelectric unicouples involves the use of different thermoelectric materials, each of which exhibits optimum performance in a different portion of the temperature range.

The figure schematically depicts a thermoelectric unicouple of the present type optimized for a source temperature of 973 K and a sink temperature of 300 K. This unicouple is made of high-performance thermoelectric materials, including (1) previously known state-of-the-art materials, (2) novel p-type alloys based on Zn_4Sb_3 and $CeFe_4Sb_{12}$, and (3) novel n-type alloys based on $CoSb_3$. Each of the p and n legs comprises segments of the various materials joined both thermally and electrically in series.

In general, the relative positions and lengths of the segments in each leg of a unicouple like this one must be chosen, taking account of the thermal conductivities of the materials, so that each segment is exposed to that portion of the source-to-sink temperature range for which the material of that segment exhibits its maximum thermoelectric performance. In addition, the ratio between the cross sections of the n and p legs must be chosen to optimize overall performance in the face of differences between the thermal and electrical conductivities in the two legs. To a first approximation (ignoring contact resistances and other relatively small effects), the energy-conversion efficiency of the unicouple depends on the ratios among the lengths of the segments but not on the overall length of the legs. However, the overall electrical and thermal resistances and the output electric power do depend on the overall length of the legs.

This work was done by Thierry Caillat, Alex Borshchevsky, Jeff Snyder, Jean-Pierre Fleurial, Andrew Zoltan, and Leslie Zoltan of Caltech for ***NASA's Jet Propulsion Laboratory****. Further information is contained in a TSP [see page 1].*

In accordance with Public Law 96-517, the contractor has elected to retain title to this invention. Inquiries concerning rights for its commercial use should be addressed to

Technology Reporting Office
JPL
Mail Stop 122-116
4800 Oak Grove Drive
Pasadena, CA 91109
(818) 354-2240

Refer to NPO-20872, volume and number of this NASA Tech Briefs *issue, and the page number.*

Microelectromechanical SPDT Switches

With respect to isolation, insertion loss, and bandwidth, these would surpass other RF switches.

NASA's Jet Propulsion Laboratory, Pasadena, California

Microelectromechanical single-pole, double-throw (SPDT) switches with predominantly planar configurations have been proposed for use in radio-frequency (RF) circuits. These switches would have overall dimensions of the order of a few millimeters and would be fabricated by micromachining techniques compatible with those used to fabricate microelectronic circuits; as such, these switches would be attractive for incorporation into inexpensive, highly integrated electronic circuits. More-

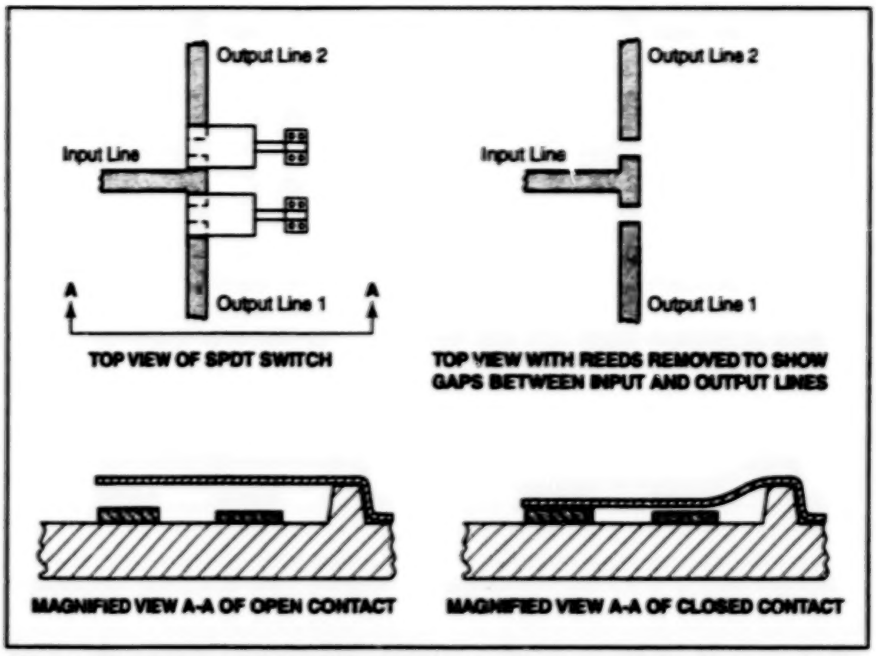
Output Line 2
Input Line
A
A
Output Line 1
TOP VIEW OF SPDT SWITCH
Output Line 2
Input Line
Output Line 1
TOP VIEW WITH REEDS REMOVED TO SHOW GAPS BETWEEN INPUT AND OUTPUT LINES
MAGNIFIED VIEW A-A OF OPEN CONTACT
MAGNIFIED VIEW A-A OF CLOSED CONTACT

Figure 1. Microelectromechanical SPDT Switches configured generally like this one would offer advantages over semiconductor switches.

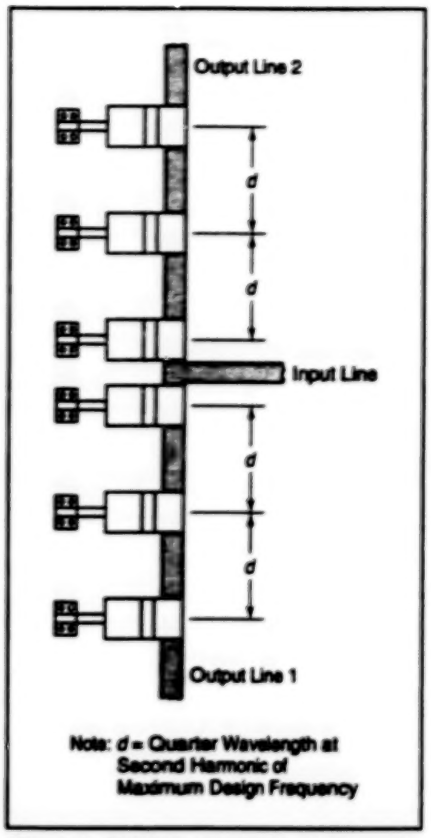

Figure 2. Multiple Contacts at Properly Designed Intervals would provide superior isolation between the input line and the "off"-side output line.

over, because of their fundamentally electromechanical character and in contradistinction to semiconductor switches, these switches are expected to exhibit minimal intermodulation distortion and very low power dissipation.

The simplest switch of this type (see Figure 1) would be an assembly of (1) a T junction between an input signal path and two output signal paths and (2) two electrostatically actuated microscopic reed contacts — one on each output path — close to the junction. In a normal operational condition, one reed contact would be closed ("on") and the other open ("off"). In this condition, the switch would provide an excellent dc and low- frequency block between the input line and the "off" output line, and an excellent conductive path between the input line and the "on" output line. However, as determined in a computational simulation, the isolation between the input line and the "off" output line at a frequency of 30 GHz would be only about 28 dB — a level that is considered mediocre in the industry.

The placement of a second reed contact directly after the first on the output lines would improve the isolation, but only by about 15 dB across most of the band from dc to the maximum design frequency (e.g., 30 GHz). A much more significant increase can be obtained placing that second contact at a quarter wavelength of 30 GHz; this would yield an improvement over the single contact case of more than 30 dB across the entire band.

The increase in isolation at 30 GHz can clearly be attributed to the impedance transformation of the second-contact open circuit to a short directly after the first contact. However, the high isolation across the rest of the band is the result of the unique circuit created by the topology. At frequencies between dc and the maximum design frequency, the open-circuited contacts and section of transmission line between them act as two very small capacitors in series with a low-pass filter between them. This low pass filter characteristic provides the high isolation at the intermediate frequencies.

Following similar reasoning, one could increase the isolation further by placing a third set of contacts at a quarter wavelength from the second contact (see Figure 2). Yet rather than placing the third contact at a quarter wavelength of the maximum fundamental frequency, if one desires to suppress second harmonic leakage, both the second and third contacts can be placed at a quarter wavelength of the second harmonic frequency to achieve an ultra-broadband, low-loss SPDT switch. This can be done with minimal effect on the performance at the fundamental frequency. For the dc-to-30-GHz case, computer simulations reveal 84 dB isolation at 30 GHz and 68 dB at 60 GHz; insertion loss at 30 GHz is predicted to be about 0.5 dB. This level of performance would exceed any other known RF SPDT switch.

This work was done by Sam Valas of Caltech for **NASA's Jet Propulsion Laboratory.** *Further information is contained in a TSP [see page 1].*

In accordance with Public Law 96-517, the contractor has elected to retain title to this invention. Inquiries concerning rights for its commercial use should be addressed to

Technology Reporting Office
JPL
Mail Stop 122-116
4800 Oak Grove Drive
Pasadena, CA 91109
(818) 354-2240

Refer to NPO-20663, volume and number of this NASA Tech Briefs issue, and the page number.

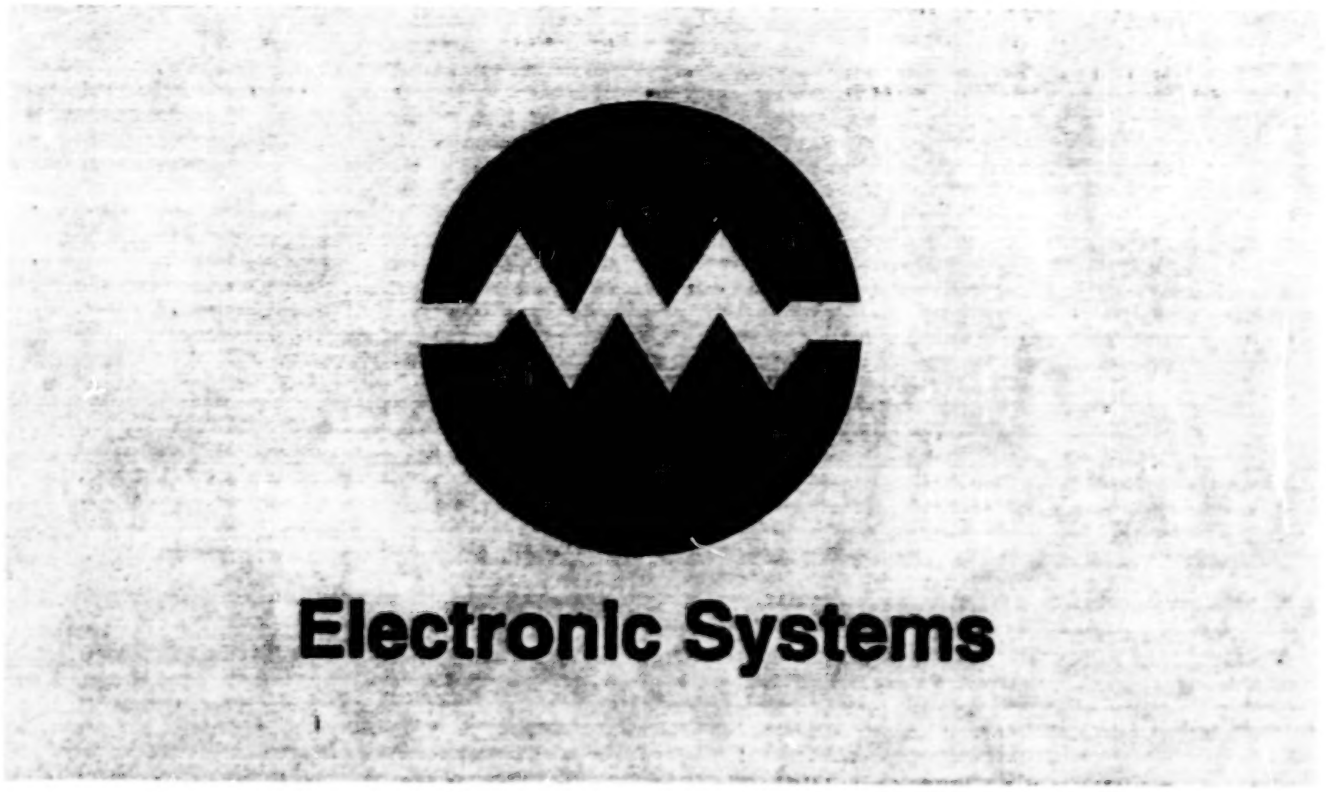

Electronic Systems

Hardware, Techniques, and Processes

11 Tunable Terahertz Source Based on Near-Infrared Diode Lasers
12 Myoelectric Teleoperation for Robotics and Prosthetics
13 Personal Cabin Pressure Alarm

BLANK PAGE

Tunable Terahertz Source Based on Near-Infrared Diode Lasers

A far-infrared signal is generated by the heterodyne method.

NASA's Jet Propulsion Laboratory, Pasadena, California

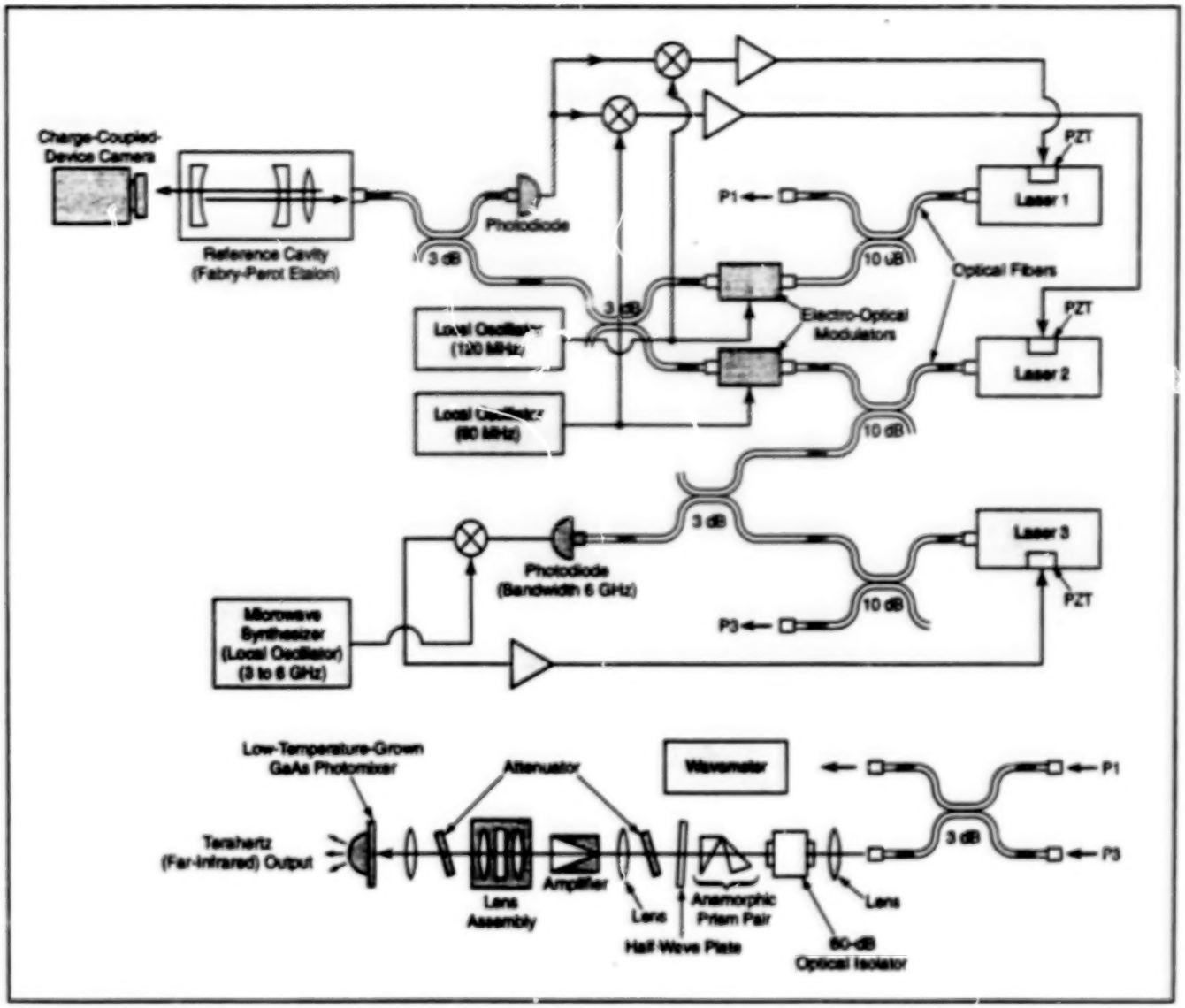

This Tunable Heterodyne Photonic Apparatus generates a spectrally narrow signal at precise frequency in the terahertz range.

The figure schematically depicts a heterodyne photonic apparatus built around three continuous-wave, near-infrared diode lasers. This apparatus generates electromagnetic radiation at an adjustable, precisely defined frequency in the terahertz range. The spectral width of the signal is less than about 1 MHz. The apparatus could serve as a prototype of tunable far-infrared sources and heterodyne up- and down-converters for fiber-optic communication systems and for testing infrared systems in general. Other potential uses lie in infrared spectroscopy for remote sensing and in research on low-energy light/matter interactions.

The three diode lasers operate at wavelengths near 850 nm. Each diode laser is packaged with a collimating lens, a resonant-cavity assembly tunable in length (and thus in frequency) by means of a piezoelectric transducer (PZT), and other optics to circularize and couple the laser output to an optical fiber. All the optical components, including the optical fibers, are polarization-maintaining.

The three diode lasers are parts of a master-oscillator subsystem that generates two laser beams at different wavelengths near 850 nm. These beams are used for two-frequency injection seeding of a single semiconductor tapered optical amplifier. The output of the amplifier is fed to a photomixer, wherein the final output terahertz signal is generated. Thus, the overall photonic system can be characterized as a photomixer pumped by a photonic master-oscillator/power-amplifier (MOPA) subsystem. Typically, the system is operated at a power-amplifier output power level of 30 mW, yielding a terahertz output power of ≈0.1 μW. At present, the output level must be limited to prevent thermal failure of the photomixer; if this limitation could be overcome, then the power amplifier could be operated at its maximum output level of 500 mW, making it possible to generate about 10 μW of terahertz output.

The frequencies of lasers 1 and 2 are controlled by locking them to different longitudinal modes of a reference cavity in the form of an ultra-low-expansion (ULE) Fabry-Perot etalon. This is accomplished by the Pound-Drever-Hall technique, which is a frequency-modulation/optoelectronic feedback control technique for stabilizing the frequency of a laser. The frequency modulation for this purpose is effected through electro-optical modulators driven at frequencies of 120 and 80 MHz, respectively.

The difference frequency between lasers 1 and 2 is discretely selectable in increments equal to the free spectral range (FSR) of the reference cavity (increments of about 3 GHz). Laser 3 is heterodyne phase-locked to laser 2, offset in frequency by an amount established by a tunable microwave synthesizer that operates in the frequency range of 3 to 6 GHz. The difference frequency between the lasers 1 and 3 — the final output frequency in the terahertz range — is the sum of the microwave offset frequency and an integer multiple of the FSR of the reference cavity. The microwave offset frequency is locked to a reference source accurate to within a fractional error $<10^{-12}$. The accuracy of the final output frequency is determined by the accuracy of measurement of the FSR (within about ±50 kHz) and by any dc offset in the electrical portions of the lock loops. The ULE material in the reference cavity has a coefficient of thermal expansion of -2×10^{-10} $(°C)^{-1}$, resulting in frequency stability (with respect to temperature) comparable to that stability of a good quartz reference oscillator in a conventional microwave source.

This work was done by Herbert Pickett, John Pearson, Serge Dubovitsky, Pin Chen, Geoff Blake, and Shuji Matsura of Caltech for **NASA's Jet Propulsion Laboratory**. *Further information is contained in a TSP [see page 1].*
NPO-20636

Myoelectric Teleoperation for Robotics and Prosthetics

Thus far, it has been possible to distinguish myoelectric signatures of two different grips.

Lyndon B. Johnson Space Center, Houston, Texas

Johnson Space Center is sponsoring continuing research on the use of myoelectric signals to control dexterous robotic and prosthetic hands. This research is expected to advance the state of the art beyond that of today's most common, commercially available, myoelectrically controlled prosthetics — clawlike devices, little altered since the 1970s, that are restricted to motion in one degree of freedom are basically motorized hooks. Thus far, the research has shown that by use of a suitable combination of electronic hardware and software, it is possible to recognize the myoelectric signatures of at least two different grips in real time, with an accuracy of at least 90 percent. While this level of performance is below the nearly 100-percent accuracy required for highly precise teleoperation (e.g., for controlling remote manipulators on the Space Station), it is high enough to offer potential benefits to the prosthetics community, and hence would be well worth further investigation. The fruits of this research might eventually include comfortable, lightweight, and relatively inexpensive prosthetic hands that could act, in a nearly lifelike manner and in real time, in response to the myoelectric signatures of as many as six different grips.

Experts in prosthetics generally agree that the following five types of grips are vital to a person's daily activities:

- The three-jaw chuck or pincher grip, used to hold small objects;
- The lateral or key grip, used to hold and actuate a key in a lock;
- The hook grip, used to carry an item like a book or a briefcase;
- The spherical grip, in which the thumb and fingers are wrapped around a sphere; and
- The cylindrical grip, in which the thumb and fingers are wrapped around a cylinder.

The designs of majority of commercially available electrical hand prostheses generally address the need for only a couple of these types of grips, and do not provide for independent control of fingers and thumbs. Most are capable of chuck grips only. Designs of the most advanced research models have provided for chuck and key grips, with options for spherical and cylindrical grips provided through passive compliance of fingers. All of these devices, at whatever level of sophistication, present control and interface problems.

One of the problems is caused by the fact that available myoelectrically controlled hands are limited to one-degree-of-freedom performance, although some offer proportional gripping forces as well. Worse yet, the most complex artificial hands are significantly larger and heavier than are human hands, and therefore amputees experience difficulty in controlling them. Indeed, the human hand is a complex mechanism that has 27 degrees of freedom and is capable of a wide range of powerful and yet delicate movements with quick, quiet, and smooth operation while exhibiting both high performance and efficiency. Therefore, it has long been thought that, given constraints on size and weight, it is well nigh impossible to design an artificial hand that performs at the level of the human hand. However, as has now been shown by the research reported here, it may be possible to construct a prosthetic hand that has multiple degrees of freedom and that performs the key motions of a human hand under control by processed myoelectric signals.

In this research, attempts were made to recognize, in real time, the myoelectric signatures of as many as six different grips by use of frequency (and, alternatively, time-frequency) techniques that "split" the signatures and by use of artificial neural networks to recognize the signatures. The development of an ability to distinguish among different grips would be a critical extension of the state of the art, inasmuch as commercially available myoelectrically controlled prostheses recognize only two usual states, i.e., "grip" and "open." In the research, various degrees of accuracy of recognition were obtained for various combinations of grips. The best results were obtained (accuracy >90 percent) in distinguishing between the chuck and key grips. Inasmuch as it was heretofore generally believed by experts in the field that it was not possible to extract grip-signature information from myoelectric signals, this is a significant achievement.

This work was done by I. D. Walker of Rice University for **Johnson Space Center**. *Further information is contained in a TSP [see page 1].*
MSC-22940

Personal Cabin Pressure Alarm

Aircraft crewmembers would be alerted to prevent hypoxia.

John F. Kennedy Space Center, Florida

Compact instruments, similar in appearance to common personal pagers, have been proposed for warning aircraft crewmembers that cabin air pressure has decreased to a potentially dangerous level. An instrument of this type, called a "personal cabin pressure monitor and warning system" (PCPMWS), implements a warning protocol consistent with Federal Aviation Administration (FAA) requirements for commercial flight crews to (1) use supplemental oxygen after a 30-minute exposure to a cabin pressure altitude between 10,000 and 12,000 ft (about 3,050 and 3,660 m), or (2) immediately when the cabin pressure altitude exceeds 12,000 ft. The PCPMWS would provide both 10,000- and 12,000-ft warnings. The elapsed time between these two warning altitudes could also serve as an indication of the rate of decompression, and thus of the urgency of the situation.

A PCPMWS is a state-of-the-art system which incorporates recent advances in sensors, low-power electronic circuitry, and high-density packaging of electronic circuitry. A production-model would be small, robust, and highly accurate. A PCPMWS contains a battery, an internal temperature-compensated pressure monitor, a microprocessor, an audio alarm, a vibrating alarm, and visual displays that would include a flashing light-emitting diode and a digital display or bar graph that would indicate the current cabin pressure altitude. The display would also serve as an indicator of the condition of the battery and functioning of the system when a momentary "TEST" button was pressed. Because a PCPMWS is a safety device, the user must depress the power switch for several seconds in order to power down the unit.

If a PCPMWS senses a cabin pressure altitude above the 10,000-ft trigger point, the audio, vibrating, and visual alarms will temporarily activate and start a 30-minute timer. If a pressure altitude between 10,000 and 12,000 ft is detected for 30 minutes or more, or immediately upon detection of a pressure altitude of 12,000 ft or more, all alarms will activate. A "TEMPORARY ALARM RESET" button will silence the alarms for 5 minutes. If the pressure condition causing the alarm is still present after the 5-minute period, the alarms will again sound. The user can configure the unit not to repeat the alarms, if so desired. Since the supplemental oxygen rules for general-aviation pilots are slightly different than for commercial operators, the unit will automatically select the applicable pressure altitude trigger points when the user selects the type of flight operation intended.

The PCPMWS is useful for both pressurized and nonpressurized aircraft operations. The device would serve as a reminder to the crew when supplemental oxygen is required for nonpressurized aircraft, and serve as a warning when the required safe cabin pressure altitude has been compromised in a pressurized aircraft. The main advantages of a PCPMWS is its portability and independence of other aircraft systems. Since the PCPMWS architecture is microprocessor-based, pressure altitude, temperature, and local pressure indications can be displayed in any convenient units of measure. Thus, it could serve as a supplemental or emergency pressure altimeter or pressure monitor for a balloon, glider, or other nonpressurized aircraft. The microprocessor could also calculate the rate of change of altitude, so that the PCPMWS could also serve as a supplemental rate-of-climb indicator.

This work was done by Jan A. Zysko of **Kennedy Space Center**. *Further information is contained in a TSP [see page 1].*

This invention is owned by NASA, and a patent application has been filed. Inquiries concerning nonexclusive or exclusive license for its commercial development should be addressed to the Technology Programs and Commercialization Office, Kennedy Space Center, (321) 867-6373. Refer to KSC-12168.

14

BLANK PAGE

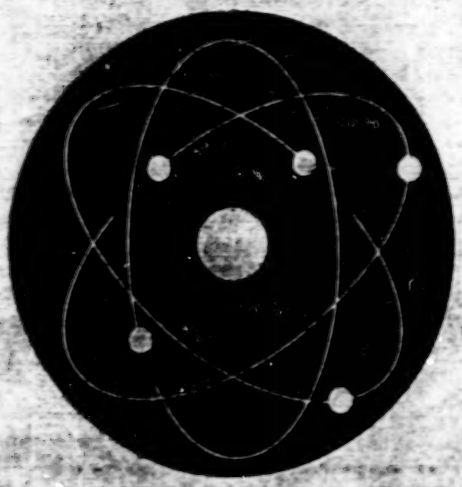

Physical Sciences

Hardware, Techniques, and Processes

17 Modifications of a Hydrazine Fueling Procedure and Equipment
18 Room-Temperature Infrared Instrument Detects Trace Gases
19 Ultrasonic Bubble-Sizing Instrument

Books and Reports

20 Tribology for Aerospace Applications
20 Surface and Gas Temperatures via Multiwavelength Pyrometry

BLANK PAGE

Modifications of a Hydrazine Fueling Procedure and Equipment

Workers could safely wear less-restrictive protective garments.

NASA's Jet Propulsion Laboratory, Pasadena, California

A combination of procedure and equipment for loading liquid hydrazine into a spacecraft fuel tank that contains a diaphragm or bladder would be modified, according to a proposal. The purpose of the modifications is to enable fueling technicians to work safely, during all but a small part of the loading process, in less-restrictive protective attire.

Heretofore, for reasons too complicated to describe in this article, the task of loading hydrazine into fuel tanks that contain diaphragms has posed such a high risk of leakage and spillage of hydrazine that technicians engaged in this task have been required to wear protective garments called Self-Contained Atmospheric Protection Ensemble (SCAPE) suits, which are bulky and which restrict movement so much as to make the simplest tasks difficult. Recently a combination of equipment and a procedure that entails the wearing of less-restrictive, less-protective splash suits has been developed; however, this combination is applicable only to tanks that do not contain diaphragms. The essence of the proposal is to modify this recently developed combination to make it safe to load a tank that contains a diaphragm while wearing splash suits instead of SCAPE suits during most of the loading process.

The proposed modifications address two concerns that bear on safety — again, for reasons too complicated to describe in this article. These concerns are the following:

1. A pressurant gas (ordinarily, helium) is used. This gas must be prevented from entering the spacecraft fuel tank on the fuel side.
2. The equipment includes, among other things, a fuel-supply tank and a transfer tube called the "flexline." Once the spacecraft fuel tank has been loaded, the flexline must be purged with the pressurant gas to blow liquid hydrazine back into the fuel-supply tank.

According to the proposal, the equipment would be modified by three additions: (1) a liquid/gas detector would be incorporated into the flexline between the fuel-supply tank and a service valve on the spacecraft fuel tank, (2) an automated valve controlled by the liquid/gas detector would be incorporated into the flexline between the service valve and the liquid/gas detector (see figure), and (3) a new purge fitting would be installed at the service valve.

The liquid/gas detector would indicate whether the flexline holds liquid hydrazine or pressurant gas. The liquid/gas detector could be a capacitance, optical-density, flotation, or other sensor. If the fuel-supply tank were to become depleted during a transfer of liquid hydrazine from the fuel-supply tank to the spacecraft fuel tank, then the pressurant gas would begin to travel along the flexline toward the spacecraft fuel tank, posing a risk that the pressurant gas might undesirably enter the spacecraft fuel tank on the fuel side. To prevent the pressurant gas from entering the spacecraft fuel tank, the liquid/gas detector would generate a command to close the automated valve as soon as it sensed the arrival of helium gas. As a result, the portion of the flexline between the liquid/gas detector and the spacecraft fuel tank would be occupied by liquid hydrazine; that is, the pressurant-gas/liquid-hydrazine front would have been prevented from traveling farther along the flexline.

At this point, it would be necessary to close the service valve: This operation would have to be performed in a SCAPE suit because there would be liquid hydrazine under pressure behind the service valve; in other words, the technicians

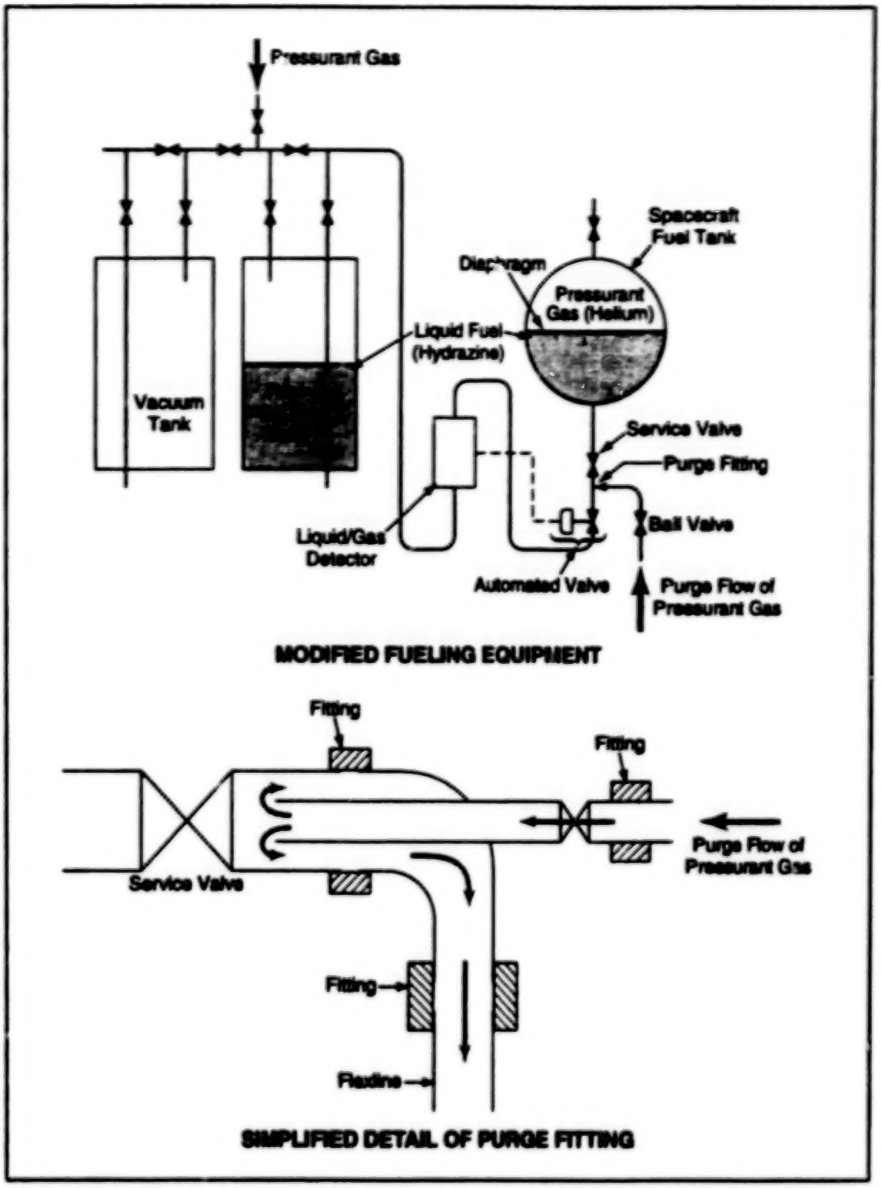

A Liquid/Gas Detector, an automated valve controlled by the detector, and a new purge fitting would be added to the equipment designed previously for loading a tank that does not contain a diaphragm.

would be only one service valve away from liquid hydrazine under pressure. Next, the liquid/gas detector would be turned off, causing the automated valve to open. The pressurant gas would then be supplied through a ball valve and the purge fitting; the flow of helium would push the liquid hydrazine in the flexline back into the fuel-supply tank. The remaining cleanup of the hydrazine-contaminated pressurant gas in the flexline could then be performed in a manner similar to that of the unmodified combination of procedure and equipment.

This work was done by John Houseman of Caltech for **NASA's Jet Propulsion Laboratory**. *Further information is contained in a TSP [see page 1].*

NPO-20679

Room-Temperature Infrared Instrument Detects Trace Gases

Times for measuring concentrations of gases can be as short as a few seconds.

Lyndon B. Johnson Space Center, Houston, Texas

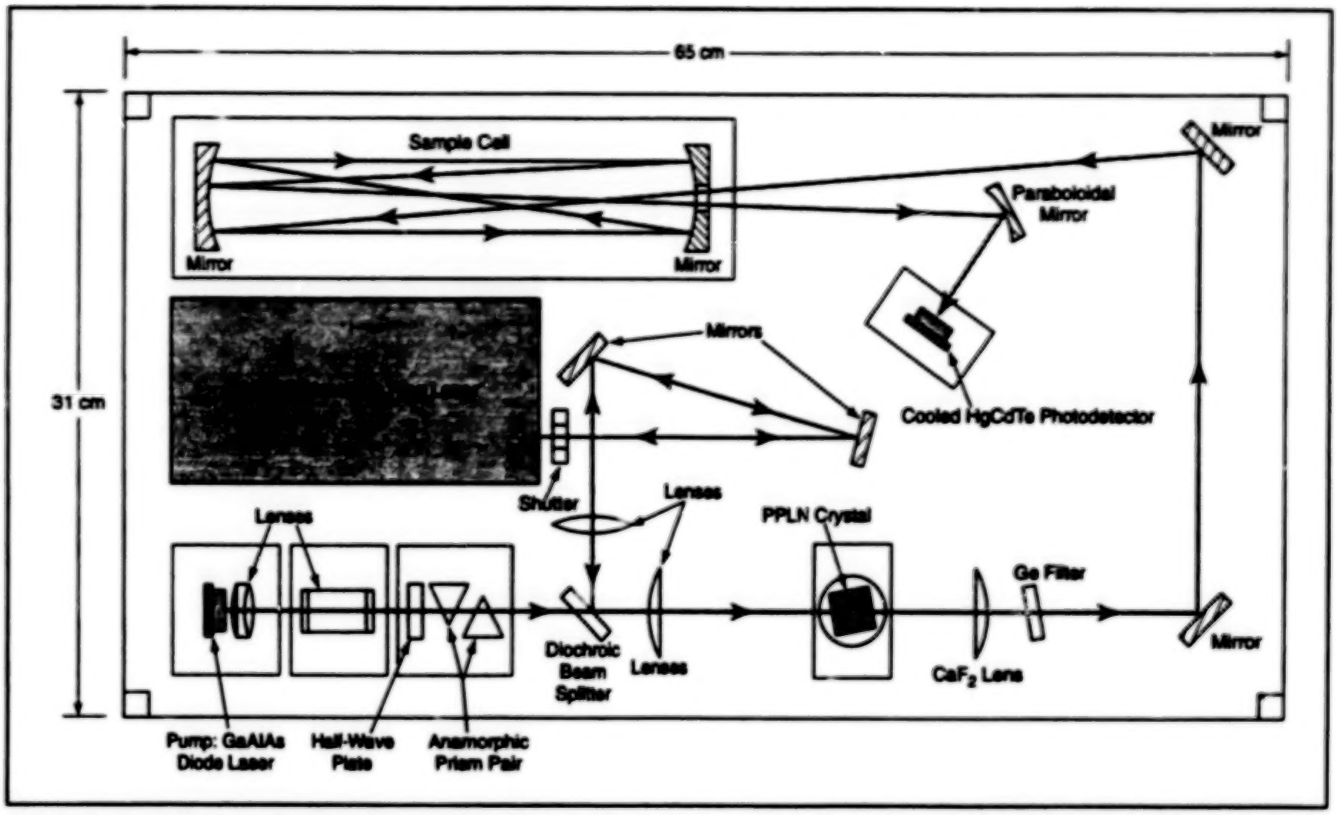

This Instrument Measures the Mid-Infrared Absorption Spectrum of a trace gas in the sample cell. The concentration of the trace gas is then computed from the measurement data.

A compact, portable, mid-infrared, laser-based instrument that operates at room temperature has been developed for use in detecting trace concentrations of CO or any of several other gases in air. The instrument utilizes infrared absorption spectroscopy in a sample cell which either holds an air sample or is exposed to an airflow. The laser beam that interrogates the cell is formed by difference-frequency generation (DFG) in a bulk nonlinear optical medium excited by two laser beams.

The figure shows the optical layout of the instrument. One of the laser injection sources is a diode-pumped, nonplanar, monolithic ring neodymium: yttrium aluminum garnet (Nd:YAG) laser with 750-mW output power at a wavelength of 1,064 nm. In the terminology of nonlinear optics, it is the 'signal' laser. Another injection source is a 100-mW GaAlAs diode laser that operates at a wavelength of 865 nm, commonly referred to as the "pump." The laser diode is packaged with a thermistor, a thermoelectric cooler, and a monitor photodiode. This choice of lasers was motivated primarily by their capability of reliable single-frequency, low-noise operation over long times in the presence of vibration and of changes in temperature and humidity.

The output of the diode laser is collimated by a multielement lens. Both the diode laser and the lens are mounted on fixtures that ensure precise long-term alignment with minimum sensitivity to vibration. After collimation, the diode-laser beam (pumping beam) passes through a compact 40-dB isolator, then through a half-wave plate, then through an anamorphic prism pair, emerging as a vertically polarized beam that is nearly mode-matched to the signal laser beam for efficient DFG.

The pump and signal beams are combined by a dichroic beam splitter and focused by a lens, at nearly normal incidence, into the nonlinear optical medium, which is an uncoated crystal of periodically poled lithium niobate (PPLN). The crystal is *z*-cut and contains eight strips with domain grating periods ranging from 22.4 μm to 23.1 μm in 0.1-μm steps. For difference-frequency mixing to produce an idler beam at a wavelength of 4.6 μm, the optimum period was found to be 22.9 μm at room temperature. The idler beam is the one that is used to probe the sample cell.

The idler beam is collimated by an

uncoated CaF_2 lens, then separated from the pump and signal beams by a germanium filter. The idler beam is then directed into the sample cell, which is a multipass cell aligned for 92 passes between mirrors separated by 20 cm to obtain an effective path length of about 18 m. The multiple passes are used to increase the measured optical absorption by the trace gas of interest, so that the trace-gas-measurement signal can substantially exceed detector noise and optical interference. An off-axis parabolic mirror collects the idler beam at the output of the cell, and focuses it onto an HgCdTe photodetector maintained at a temperature of –65 °C by a three-stage Peltier cooler. In the output of the photodetector, absorption signals take the form of amplitude modulation. The output of the detector is digitized by a data-acquisition card that serves as an interface to a laptop computer. The card is also used to control a small mechanical shutter to block the signal beam for 10 seconds every three minutes for taking "dark" readings.

The spectroscopic information collected by the computer consists of the photodetector output voltage as a function the laser-frequency-control voltage (the signal used to control the current supplied to the diode laser and thereby control the pump wavelength). A time trace of the photodetector output voltage is a function of time averaged over 10 to 1,000 sweeps minus dark voltage. The time trace can be converted to a wavelength trace, once the pump frequency as a function of time is known. Depending on the number of sweeps used to generate the average, the spectrum can be updated at intervals that range from 1 to 20 seconds. At any point in the frequency scan, the concentration of the absorbing gas species of interest can be calculated by applying the Beer-Lambert law.

The entire instrument including power supplies and electronics is contained in an aluminum case that measures 31 by 31 by 65 cm. The instrument draws less than 50 W of electric power and can be operated from car batteries. The instrument has been shown to be capable of detecting CO in air at atmospheric pressure at mole fractions as low as 100 parts per billion, with a precision of 1 part per billion and an accuracy of 0.6 percent at an averaging time of 10 seconds. The use of a diode laser equipped with an external cavity could enable tuning over a wave-number range of 700 cm^{-1}, making it possible to detect several trace gases, including N_2O, CO_2, SO_2, H_2CO, and CH_4.

This work was done by Konstantin P. Petrov, Robert F. Curl, and Frank K. Tittel of Rice University for **Johnson Space Center**. *Further information is contained in a TSP [see page 1].*

This invention is owned by NASA, and a patent application has been filed. Inquiries concerning nonexclusive or exclusive license for its commercial development should be addressed to the Patent Counsel, Johnson Space Center, (281) 483-0837. Refer to MSC-22864.

Ultrasonic Bubble-Sizing Instrument

Bubbles associated with decompression sickness can be detected noninvasively.

Lyndon B. Johnson Space Center, Houston, Texas

An ultrasonic instrument has been developed for measuring the sizes of bubbles in the human body. A primary example is that of bubbles associated with decompression sickness (the "bends"); these bubbles consist mostly of nitrogen and can occur in both blood vessels and extravascular tissues. The bubbles can lodge (embolize) in vessels in the lungs and elsewhere, causing any of a variety of pathological conditions. Gaseous emboli that cause decompression sickness pose a serious risk of injury to aviators, astronauts, divers, and other individuals who are exposed to varying environmental pressures. Gaseous emboli can also be serious complications of cardiopulmonary bypass operations, introduction of air during cardiotomy, and cavitation bubbles generated by replacement heart valves.

The present instrument can be expected to aid research on decompression sickness and other gaseous embolic events by providing a capability to: (1) distinguish between gaseous and thrombotic emboli, and (2) measure the sizes of gaseous emboli noninvasively. It could be useful in research on heart valves, development of coronary-bypass machines, and cardiotomy.

The physical basis of the instrument is the use of ultrasound to excite the resonant behavior (oscillatory expansion and contraction) of gaseous emboli. The resonant behavior is a function of the bubble diameter and has been well characterized analytically, so that little or no calibration of the instrument is needed. Nongaseous (e.g., thrombotic) emboli do not display the same resonant characteristics as do gaseous emboli; this difference can be a means for distinguishing between the two types of emboli.

The instrument includes several ultrasonic transducers. One of them, denoted the pump transducer, is driven at a relatively low ultrasonic frequency (f_p) and is used to excite the fundamental vibrational mode of any bubbles that may be present. The other transducers are operated at a higher carrier frequency (f_i) in a pulse/echo mode and are part of an ultrasonic imaging subinstrument used to observe bubbles as they resonate. The instrument also includes signal-processing and -analysis equipment.

To interrogate the measurement volume for a particular bubble size, one simultaneously insonifies the measurement volume with (1) a pump signal with f_p set at the resonance frequency for that bubble size and (2) the higher-frequency imaging signal. Properly excited, the bubbles respond nonlinearly to the ultrasonic signals. In this case, they act as signal mixers; consequently, measurable signals at $f_i + f_p$ and $f_i - f_p$ are present in the high-frequency return signal if and only if there is a gaseous bubble with a fundamental resonance frequency equal to f_p. The range of bubble sizes of interest is scanned by varying f_p frequency over the appropriate range.

This work was done by Patrick J. Magari, Robert Kline-Schoder, and Brant Stoedefalke of Creare, Inc., for **Johnson Space Center**. *Further information is contained in a TSP [see page 1].*

This invention is owned by NASA, and a patent application has been filed. Inquiries concerning nonexclusive or exclusive license for its commercial development should be addressed to the Patent Counsel, Johnson Space Center, (281) 483-0837. Refer to MSC-22980.

Books and Reports

Tribology for Aerospace Applications

"Tribology for Aerospace Applications" is a textbook and reference source written for designers of rotating machinery; users and designers of such mechanical components as bearings, gears, and seals; tribologists; university and industrial researchers; and students of machine design. The book was conceived to satisfy a need, expressed by members of a world-class tribology and mechanical components research group at the former Lewis Research Center (now Glenn Research Center), to preserve and extend the knowledge gained through their work. The book incorporates information from more than 900 references spanning over 50 years of technological advances. The contents of the references, ranging from classical topics in tribology to cutting-edge technology now used by the aerospace community, have been digested, reinterpreted, and integrated into ten chapters. Each chapter could be a book in itself if published separately. The titles of the chapters are "Tribology Fundamentals," "Solid Lubricants," "Self-Lubricating Polymer Composites," "Liquid Lubricants," "Traction Lubricants," "Rolling Bearing and Gear Lubrication," "Rolling Bearing and Gear Materials," "Fluid and Gas Film Lubrication," "Engine Seals," and "System Life and Reliability." The book also contains a glossary, plus appendices entitled "Model Specifications for Rolling Bearings" and "Model Engineering Drawings for Rolling Bearings."

This book was coauthored and edited by Erwin V. Zaretsky of **Glenn Research Center** *in collaboration with the staff of Glenn Research Center and the Society of Tribologists and Lubrication Engineers. Copies of the book can be ordered from Society of Tribologists and Lubrication Engineers, 840 Busse Highway, Park Ridge, IL 60068-2376; telephone (847) 825-5536; fax (847) 825-1456.*

Inquiries concerning rights for the commercial use of this invention should be addressed to NASA Glenn Research Center, Commercial Technology Office, Attn: Steve Fedor, Mail Stop 4–8, 21000 Brookpark Road, Cleveland, Ohio 44135. Refer to LEW-17028.

Surface and Gas Temperatures via Multiwavelength Pyrometry

A report describes experiments using multiwavelength pyrometry to determine the surface temperature of the end tip inside a BeO cylinder that is part of a probe designed to measure high-temperature gases. The cylinder is heated by the gas into which it is inserted, and the gas temperature is related to the tip temperature via a mathematical model of the probe. In multiwavelength pyrometry, plotting the radiant temperatures derived from experimental data according to Planck's law results in a straight line, the intercept of which at zero wavelength is the reciprocal of the desired temperature. [This procedure was described in more detail in "Measuring Temperature of Glass by Multiwavelength Pyrometry" (LEW-16614), *NASA Tech Briefs*, Vol. 22, No. 11 (November 1998), page 36.] The probe was tested in two atmospheric burner experiments. The measured interior temperatures were 1,360 and 1,745 K. Available temperature information on the burner flame is lower, being at 1,300 and 1,580 K, respectively. This was so because the thermocouples performing the measurement were positioned at the cooler periphery of the jet to avoid being destroyed by hot gases at the burner's central flow, the hot temperature of which the BeO probe was successful in measuring.

This work was done by Gustave Fralick and Daniel Nig of **Glenn Research Center**. *To obtain a copy of the report, "Pyrometric Gas and Surface Temperature Measurements," see TSP's [page 1].*

Inquiries concerning rights for the commercial use of this invention should be addressed to NASA Glenn Research Center, Commercial Technology Office, Attn: Steve Fedor, Mail Stop 4–8, 21000 Brookpark Road, Cleveland, Ohio 44135. Refer to LEW-16972.

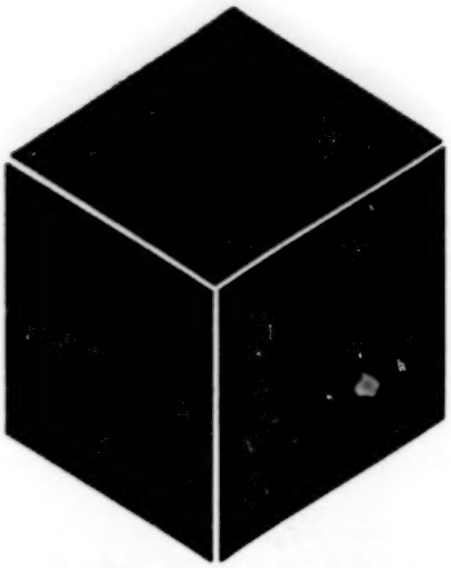

Materials

Hardware, Techniques, and Processes

23 Graphite/Conductive-Epoxy Electromagnetic Shielding
23 SiC/SiC Composites With Improved BN Coating on Fibers
24 Silica-Filled EPDM Rubbers as Ablative Insulating Materials
24 Carbon-Filled EPDM Rubbers as Ablative Insulating Materials
25 Composite-Material Pipes for Corrosive and Cryogenic Liquids
25 Making Submicron Features by Ion Etching Through PMMA Masks
26 Reactive-Ion Etching of Smooth Vertical Walls in Silicon

Books and Reports

26 Development of Progressive-Failure-Analysis Software

BLANK PAGE

Graphite/Conductive-Epoxy Electromagnetic Shielding

Shielding ability equals that of a larger mass of aluminum.

John H. Glenn Research Center, Cleveland, Ohio

Lightweight shields for electromagnetic interference (EMI) can now be fabricated from composites of (1) electrically conductive fibers made of bromine-intercalated graphite in (2) matrices of electrically conductive epoxy. As shown in more detail below, the shielding ability of a given thickness of this composite material equals that of a greater thickness of aluminum.

Electrical conductivity of surface layers is essential for EMI shielding. Previously, NASA had developed EMI shields made of bromine-intercalated graphite fibers in matrices of electrically insulating epoxy. However, those shields were not as effective as aluminum shields because of the lack of electrical conductivity in the epoxy (especially in surface layers).

The table compares the shielding effectiveness of a sheet of aluminum and a sheet of the present bromine-intercalated-graphite-fiber/electrically-conductive-epoxy composite. On the basis of performance figures like those in this table, it has been estimated that by use of this composite material, it should be possible to make EMI shields thinner than aluminum shields (which are typically about 2 mm) but equally as strong and equally as effective against EMI. It has been further estimated that reductions in weight, relative to aluminum shields, can be expected to lie between 34 and 88 percent.

Aluminum	~80	~42.9
Composite of Bromine-Intercalated Fibers in a Matrix of Electrically Conductive Epoxy	~80	~24.2

The EMI-Shielding Performance of a 2-mm thick sheet of aluminum and a 0.36-mm thick sheet of the present composite material made from electrically conductive epoxy were measured at frequencies of 10 and 35 GHz.

This work was done by John D. Lennhoff and George G. Harris of Triton Systems, Inc., for **Glenn Research Center.** *Further information is contained in a TSP [see page 1].*

Inquiries concerning rights for the commercial use of this invention should be addressed to NASA Glenn Research Center, Commercial Technology Office, Attn: Steve Fedor, Mail Stop 4–8, 21000 Brookpark Road, Cleveland, Ohio 44135. Refer to LEW-16647.

SiC/SiC Composites With Improved BN Coating on Fibers

The in-situ BN coating helps to deflect cracks away from the fibers.

John H. Glenn Research Center, Cleveland, Ohio

A method of fabricating composites of pretreated silicon carbide fibers in silicon carbide matrices provides for the formation of improved boron nitride fiber/matrix interfacial layers. As explained below, these BN layers help to deflect matrix cracks away from the fibers.

In order to impart strength and fracture toughness to a fiber/matrix composite material, one must formulate it so that under high stress, it fails in a fiber-pullout mode rather than a brittle-fracture mode. This requirement translates to a need for a fiber/matrix interfacial layer of a material (denoted the "interphase") that is weakly bonded to both the fibers and the matrix to insure that matrix cracks are deflected away from the fibers.

One of the most widely used fiber/matrix interphases is boron nitride, which, heretofore, has usually been deposited on fibers or fiber preforms by chemical vapor deposition (CVD). One of the drawbacks of the CVD BN process is that when a tow (a bundle that normally consists of between 500 and 800 fibers with diameters between 10 and 15 μm) is formed into a woven fiber preform prior to CVD BN coating, many of the fibers are in contact with each other and therefore do not become completely coated with BN. On subsequent fracture of the composite, those fibers that are in contact with no BN between them tend to fail in a brittle manner, with little or no fiber pullout. This situation is exacerbated if the SiC fibers have relatively rough surfaces (as some commercial SiC fibers do). In addition, ordinary CVD BN fiber coats are not particularly crystalline, and have been found to be very susceptible to oxidation in hot, moist environments like those in gas turbine combustors.

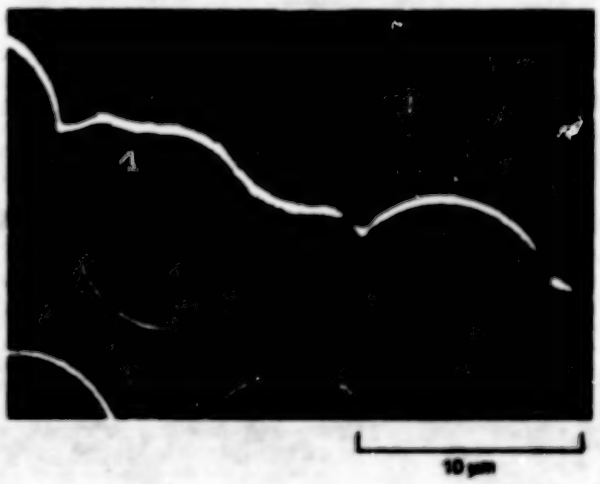

A Matrix Crack Has Been Diverted Around Three Fibers at the interfaces between (1) the highly crystalline *in situ* BN layers and (2) the CVD BN layers at the fiber/matrix interfaces.

In the present method, thin layers of either (1) carbon-rich SiC containing some boron or (2) highly crystalline BN are formed *in situ* on the SiC fibers, before fur-

ther processing; these layers prevent the SiC fibers from remaining in contact with each other. Because these thin surface layers are not thin enough (and, in the case of highly crystalline BN are not weak enough) to act by themselves as crack-deflecting layers, it is necessary to deposit BN overcoats (with or without Si doping) by chemical vapor infiltration to obtain the desired crack-deflection property. The remaining processing steps, following conventional practice, include the formation of SiC overcoats by chemical vapor infiltration, infiltration by a slurry that contains SiC particulate, and infiltration by molten silicon at a temperature of ≈1,420 °C to realize a dense matrix.

The subprocess to form the boron-doped carbon or highly crystalline BN begins with a heat treatment of the fibers at a temperature of 1,800 °C in either an inert or nitrogen gas. In the case of a nitrogen atmosphere, boron (which is present in typical commercial SiC fibers as a sintering aid) diffuses to the fiber surfaces to form thin (≈100- nm thick) layers of very crystalline BN. The added advantage of diffusing the boron out of the fibers is that the resistance to creep of the fibers at high temperatures is increased. In the case of an inert atmosphere, the surfaces of the fibers become reduced, with resultant formation of thin (≈50 to ≈100 nm thick) carbon-rich surface layers, which also contain some boron from diffusion out of the bulk.

When the fibers that have been thus heat treated are subsequently woven into cloth preforms or are heat-treated in cloth form, the highly crystalline BN or carbon-rich surface layers prevent the SiC fiber cores from touching. While carbon-rich fiber surface layers may prevent the fibers from touching, they are not desired because they do not exhibit sufficient resistance to oxidation as that of the BN layers.

The highly crystalline layers of BN are strongly bonded to the fiber surfaces, and prevent the propagation of cracks from the matrix into the fibers (see figure). By keeping the fibers out of contact, the highly crystalline layers also prevent interlocking of the rough fiber surfaces. The highly crystalline nature of these layers also contributes to stability under stress in an oxidizing environment.

This work was done by James A. DiCarlo and Hee Mann Yun of **Glenn Research Center** *and John J. Brennan of United Technologies. Further information is contained in a TSP [see page 1].*

Inquiries concerning rights for the commercial use of this invention should be addressed to NASA Glenn Research Center, Commercial Technology Office, Attn: Steve Fedor, Mail Stop 4–8, 21000 Brookpark Road, Cleveland, Ohio 44135. Refer to LEW-16864.

Silica-Filled EPDM Rubbers as Ablative Insulating Materials

These materials are intended to replace other materials that will soon be unavailable.

Marshall Space Flight Center, Alabama

Silica-filled polymers made from ethylene propylene diene monomer (EPDM) have been found to be useful as ablative thermal-insulation materials. These polymers have been investigated as candidates to replace some previously developed polymeric ablative rocket-engine insulating materials that will soon become commercially unavailable. Although these materials have been developed specifically for use in and on solid-fuel rocket motors, they may also be useful in terrestrial applications in which there are requirements for protection against high temperatures for short times.

Several formulations of silica-filled EPDM polymers have been investigated. These formulations incorporate improvements where possible. Examples of improvements include the use of a tackifier or the choice of one or more accelerator(s) to obtain a longer scorching time as well as desired curing properties. For each formulation, the ingredients are mixed according to ordinary rubber-processing techniques in a two-pass mixing procedure implemented in an internal mixer. All the ingredients except the accelerator(s) and sulfur (if used) are added during the first pass; the accelerators and sulfur (if used) are added during the second pass. In ablative tests, some formulations unexpectedly performed better than others did.

This work was done by David G. Gullot of Thiokol Corp. for **Marshall Space Flight Center.** *For further information, please contact the company at gulldg@thiokol.com.*

Title to this invention has been waived under the provisions of the National Aeronautics and Space Act [42 U.S.C. 2457(f)] to Thiokol Corporation. Inquiries concerning licenses for its commercial development should be addressed to

Thiokol Propulsion
Intellectual Property Department
PO Box 707
M/S A11
Brigham City, UT 84302-0707

Refer to MFS-31406, volume and number of this NASA Tech Briefs *issue, and the page number.*

Carbon-Filled EPDM Rubbers as Ablative Insulating Materials

These materials are intended to replace other materials that will soon be unavailable.

Marshall Space Flight Center, Alabama

Carbon-fiber-filled polymers made from ethylene propylene diene monomer (EPDM) have been found to be useful as ablative thermal-insulation materials. Like the silica-filled EPDM polymers described in the preceding article, these polymers have been investigated as candidates to replace some previously developed polymeric ablative rocket-engine insulating materials that will soon become commercially unavailable.

Several formulations of carbon-fiber-filled EPDM polymers have been investigated. As in the case of the silica-filled polymers described in the preceding article, improvements are incorporated where possible and examples of improvements include the use of a tackifier or the choice of one or more accelerator(s) to obtain a longer scorching time as well as desired curing properties. For each formulation, the ingredients are mixed in the following procedure:

First, the ingredients are mixed according to ordinary rubber-processing techniques in a two-pass mixing procedure implemented in an internal mixer. All the ingredients except the accelerator(s) and sulfur (if used) are added during the first

pass, and the accelerators and sulfur (if used) are added during the second pass. The resulting mixture is dissolved in a suitable solvent such as hexane. The solution is then mixed with carbon fibers, using a minimum of mixing to disperse the fibers and distribute them uniformly without breaking them excessively. The solution/fiber mixture is then spread thin on a flat sheet so that the solvent can evaporate (if desired, evaporation can be done in an oven). The resulting uncured insulating material is then cured in the required shape.

In ablative tests, some of the formulations investigated performed a little better than others did, probably because of differences in mixing.

This work was done by David G. Gullot of Thiokol Corp. for **Marshall Space Flight Center**. *For further information, please contact the company at gullidg@thiokol.com.*

Title to this invention has been waived under the provisions of the National Aeronautics and Space Act (42 U.S.C. 2457(f)) to Thiokol Corporation. Inquiries concerning licenses for its commercial development should be addressed to

Thiokol Propulsion
Intellectual Property Department
PO Box 707
M/S A11
Brigham City, UT 84302-0707

Refer to MFS-31405, volume and number of this NASA Tech Briefs *issue, and the page number.*

Composite-Material Pipes for Corrosive and Cryogenic Liquids

Piping systems with complex shapes can readily be fabricated.

Marshall Space Flight Center, Alabama

A flexible design concept and an associated method of fabrication have been conceived as means to satisfy growing demands for lightweight composite-material pipes for corrosive and cryogenic liquids. The design concept and method can be applied to produce piping systems capable of handling such diverse liquids as cryogenic oxygen, hydrogen peroxide, strong acids, and strong bases. The piping systems can be complex; for example, they can include manifolds and/or pipes with multiple bends.

Fabrication begins with the molding and/or machining structural segments in basic shapes that can be assembled into a mandrel that defines the geometry of a complex piping system. The basic shapes can include elbows, T junctions, Y junctions, and flanges.

Once the shapes have been joined to form a mandrel, various composite-material layers are deposited on the mandrel to form the piping. The first layer to be deposited on the mandrel is a liner. The liner can be a single thin layer of a metal, a metal layer comprising thin sublayers of different metals, or a polymer, for example.

Multiple layers of a composite material are placed on the liner and cured. The mandrel material is then removed from inside, leaving a thin-walled composite tube structure. Next, the structure is covered by a thermal-insulation layer. If the liquid to be contained is cryogenic, then a suitable insulating material could be low-density polyurethane foam; if the liquid to be contained is hot, then a better insulating material would be a phenolic fire-resistant foam. The foam can be sprayed and later machined; alternatively, premachined foam segments can be assembled onto the piping. If needed, small channels can be machined in the foam layer to accommodate a cooling or heating manifold.

The foam layer is covered with an outer composite-material skin. Finally, the structure is heated to cure the resin in the skin.

This work was done by Thomas K. DeLay of **Marshall Space Flight Center**.

This invention is owned by NASA, and a patent application has been filed. For licensing inquiries, contact Sammy Nabors, MSFC Commercialization Assistance Lead, at (256) 544-5226 or sammy.nabors@msfc.nasa.gov. Refer to MFS-31381.

Making Submicron Features by Ion Etching Through PMMA Masks

The proper choice of materials and process parameters is critical to success.

NASA's Jet Propulsion Laboratory, Pasadena, California

Experiments have shown that a substrate can be patterned with submicron features by the following procedure:

1. Coat the substrate with a layer of poly(methyl methacrylate) [PMMA], which will serve as an electron-beam resist to be patterned into an etch mask.
2. Pattern the PMMA by electron-beam lithography.
3. Ion-etch through the PMMA to transfer the pattern to the substrate.

The procedure has been used to fabricate a 600-nm-pitch diffraction grating; it could also be used to form submicron features on semiconductor and other devices.

Prior to the development of this procedure, it was known that submicron features can be produced in a PMMA resist by exposing it to an electron beam, then developing it. However, the transfer of submicron features from a PMMA mask to a substrate by either dry or wet etching had not been demonstrated. As a result of the development of the present procedure, it is now known that success in the transfer of submicron features depends on the proper choice of the substrate material(s), the thicknesses of the substrate and PMMA, the etching method, and the etching conditions.

The substrate for 600-nm-pitch grating was a 100-nm-thick gold film on a 5-nm-thick chromium layer on a quartz disk; the Cr and Au films were deposited on the disk in an electron-beam evaporation system. A PMMA resist 120 nm thick was spun onto the Au surface.

The 600-nm-pitch grating pattern was imparted to the PMMA by use of an electron-beam lithography machine. The electron-beam dose in the exposed regions was about 200 $\mu C/cm^2$, and the beam current was 5 nA. Following the electron-beam exposure, the pattern in the resist was developed by use of a 1:3 mixture of methyl isobutyl ketone and isopropyl alcohol.

The ion etching technique used to transfer the pattern to the substrate could be characterized, more precisely, as milling by a beam of argon ions. The etching was performed in argon-ion-milling system that included an ion-beam source in a vacuum chamber that was capable of evacuation to a base pressure of 4×10^{-6} torr (~5 μPa).

During operation of the ion-beam source, the pressure of argon in the system was raised to 2×10^{-4} torr (≈0.03 Pa) by addition of argon gas to the chamber at a controlled rate. This operating pressure was chosen to be high enough to generate a sufficient population of ions to obtain the desired beam current density, but not so high that the beam would be excessively dispersed through collisions with gas molecules.

The ion-beam-generating potential was 1.5 kV. The total beam current was 10 mA. The beam was spread over a cross section approximately 5 cm in diameter. The etching time was about 2 minutes.

This work was done by Thomas George, Richard Muller, Paul Maker, and David Bansic of Caltech for **NASA's Jet Propulsion Laboratory**. *Further information is contained in a TSP (see page 1).*

NPO-20649

Reactive-Ion Etching of Smooth Vertical Walls in Silicon

These walls are suitable for low-loss optical waveguides.

NASA's Jet Propulsion Laboratory, Pasadena, California

An advanced technique of deep reactive-ion etching (DRIE) has been developed for fabricating smooth vertical walls in silicon wafers. These walls are suitable for use as bounding surfaces of optical waveguides in photonic and optoelectronic devices. The roughness of a typical 8-μm-high vertical wall surface of a waveguide made by this technique is <20 nm; by keeping the roughness at such a low level, one helps to ensure that the waveguide is capable of low-loss optical transmission.

The specific DRIE technique, denoted the "Boesch" technique, involves repeated exposure of a photoresist-masked silicon wafer to (1) an etchant ($SF_6 + C_4F_8$) plasma in alternation with a passivant (C_4F_8) plasma. To ensure vertical, smooth walls, it is necessary to investigate, in detail, the effects of variations in all photoresist and DRIE process parameters and then to exert tight control over these parameters. Among other things, this means that the photoresist process parameters must be chosen to obtain perpendicular photoresist side walls. The power levels of the plasma apparatus in the etching and passivating steps, the durations of these steps, the total number of etching-and-passivating cycles, and the pressures and rates of flow of the SF_6 and C_4F_8 gases must also be investigated in detail and then controlled to obtain vertical walls with low roughness.

Ranges of parameters that have been investigated in a DRIE apparatus at NASA's Jet Propulsion Laboratory are the following:

- Total process time — 10 to 30 minutes;
- Pressure — 5 to 40 millitorr (0.7 to 5 Pa)
- Durations of etching and passivating steps — 4 to 10 seconds;
- Rate of flow of SF_6 gas during etching step — 100 to 180 standard cubic centimeters per minute (sccm);
- Rate of flow of C_4F_8 gas during etching step — 30 to 70 sccm;
- Platen power during etching step — 12 to 16 W;
- Coil power during etching step — 575 to 650 W;
- Rate of flow of C_4F_8 during passivating step — 90 to 140 sccm;
- Platen power during passivating step — 0 to 2 W;
- Coil power during passivating step — 575 to 650 W.

This work was done by Chi Wu, Stephen Vargo, and Tashe Turner of Caltech for **NASA's Jet Propulsion Laboratory**. *Further information is contained in a TSP (see page 1).*

In accordance with Public Law 96-517, the contractor has elected to retain title to this invention. Inquiries concerning rights for its commercial use should be addressed to

Technology Reporting Office
JPL
Mail Stop 122-116
4800 Oak Grove Drive
Pasadena, CA 91109
(818) 354-2240

Refer to NPO-20756, volume and number of this NASA Tech Briefs issue, and the page number.

Books and Reports

Development of Progressive-Failure-Analysis Software

A report discusses the development of the GENOA-PFA computer program, which was described in "Software for Simulating Progressive Fracture in Braided PMCs" (LEW-16845), *NASA Tech Briefs*, Vol. 24, No. 3 (March 2000), page 52; and "Update on a Progressive-Failure-Analysis Software System (LEW-16858)" *NASA Tech Briefs*, Vol. 24, No. 7 (July 2000), page 67. To recapitulate: GENOA-PFA (a commercial version of the CODSTRAN program) implements a progressive-failure methodology. On the bases of material-property data, finite-element mathematical models, and service conditions, GENOA-PFA simulates the progression of damage ultimately leading to fractures in matrix/fiber composite materials, including complex ones in which the fibers are incorporated in two- or three-dimensional weaves or braids. The first chapter of the instant report summarizes the present state of development. The remaining chapters present details of the progressive-failure methodology, mathematical modeling, and computational implementation: topics include modularization of CODSTRAN; adaptive refinement of computational meshes; progressive fracture under cyclic fatigue; simulation of the shaping of composite preforms during manufacturing; probabilistic failure analysis; mechanics of three-dimensional woven, braided, and stitched composites; effects of impacts on such composites; and the GENOA graphical user interface.

This work was done by Frank Abdi of Alpha Star Corp. and Levon Minnetyan of Clarkson University for **Glenn Research Center**. *To obtain a copy of the report, "Development of GENOA Progressive Failure Parallel Processing Software Systems," see TSP's (page 1).*

Inquiries concerning rights for the commercial use of this invention should be addressed to NASA Glenn Research Center, Commercial Technology Office, Attn: Steve Fedor, Mail Stop 4–8, 21000 Brookpark Road, Cleveland, Ohio 44135. Refer to LEW-17045.

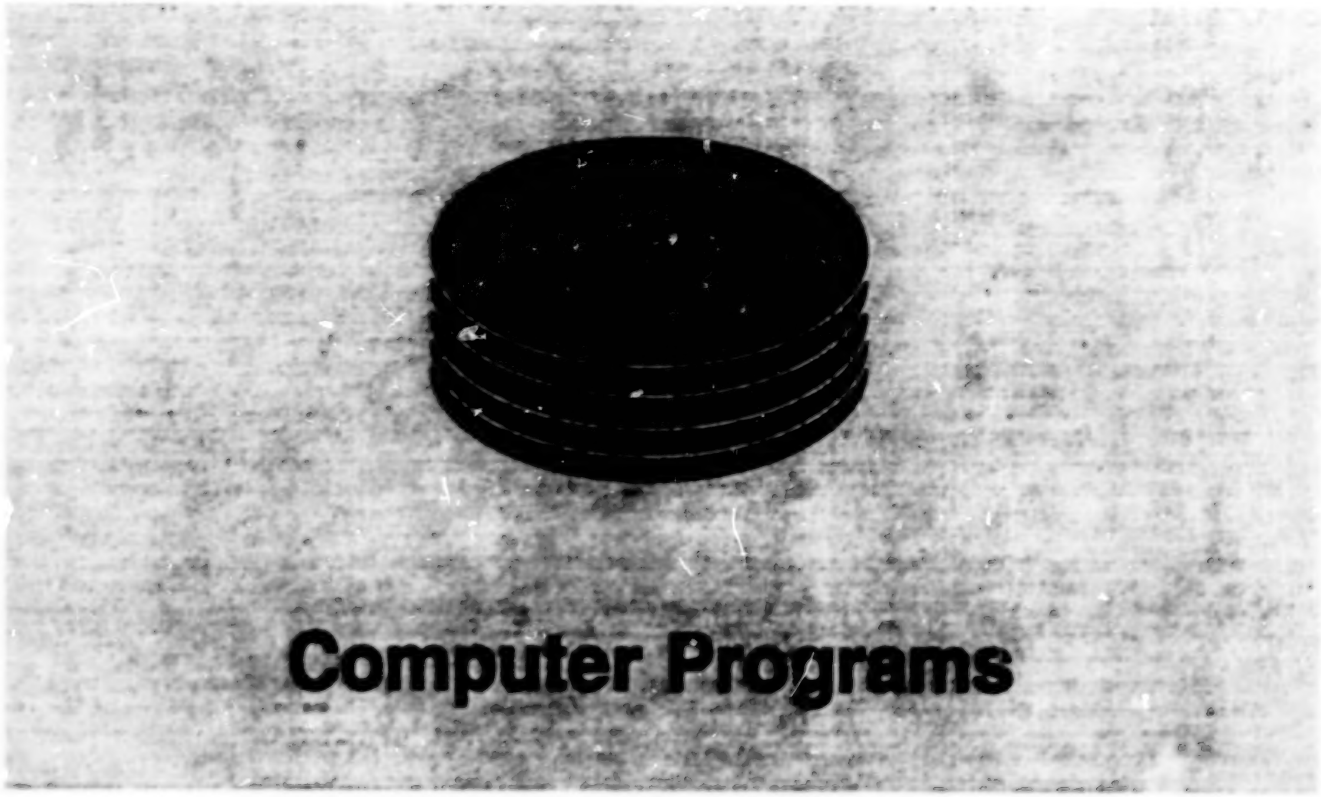

Computer Programs

Mechanics

29 Software Predicts Noise From Rotor-Wake/Stator Interactions

Mathematics and Information Sciences

29 Software for Obtaining Ideal SAR Chirps

ANK PAGE

Mechanics

Software Predicts Noise From Rotor-Wake/Stator Interactions

V072 is a computer program that predicts the noise generated by the interaction between the rotor-blade wake (fan wake) and the stator vanes of a turbofan engine. The program is a combination of subroutines from prior NASA programs, with many added features.

Limits on aircraft noise near airports are becoming more stringent. Noise associated with fans is a significant portion of the noise that emanates from modern turbofan engines. In order to reduce noise from fan stages, engineers rely on accurate computer programs to predict noise from new blading and duct designs. V072 is useful because it quickly predicts inlet and aft sound-pressure and power levels.

In V072, the computation of noise is divided into two parts: a rotor-wake calculation and the stator-noise-response calculation. First, V072 uses a semiempirical mathematical model of a wake to calculate the characteristics of the rotor wake at the leading edge of the stator. The fan stage is modeled as a constant-area annulus with the rotor blades and stator vanes represented as twisted flat plates. Empirical rotor-wake profiles are superimposed on a two-dimensional, analytically calculated mean flow. The wake model can be augmented by simple tip- and hub-vortex models. Wake harmonic magnitudes and amplitudes are then calculated at the leading edge of the stator.

The results from the wake-model calculation are then automatically fed as input to an analytical noise-prediction routine. More specifically, the unsteady flow predicted in the wake-model calculation is used to calculate the total harmonic power levels propagating upstream and downstream in the engine duct. The noise-prediction routine calculates inlet and aft sound-pressure and power levels for the blade-passage-frequency tones and their harmonics, along with complex radial mode amplitudes. The code can calculate the noise from either a fan-wake/outlet-guide-vane interaction or a fan-wake/core-stator interaction.

Although V072 is based partly on many simplifying assumptions about the fan geometry and the flow through the fan stage, V072 is nevertheless a useful software tool for designing to minimize fan noise. (The simplifications incorporated in the code make it unsuitable for analyzing cases that involve transonic or supersonic fan-tip speeds.) This program runs quickly on modern Unix workstations, making it possible to predict noise for many new designs in a timely manner, and thereby reducing the number of experiments needed to prove noise-reduction concepts.

This program was written by David Topol and Douglas C. Mathews of United Technologies for **Glenn Research Center**. *For further information on this code, please visit the following web site: http://www.grc.nasa.gov/WWW//5900/5940.*

Inquiries concerning rights for the commercial use of this invention should be addressed to NASA Glenn Research Center, Commercial Technology Office, Attn: Steve Fedor, Mail Stop 4–8, 21000 Brookpark Road, Cleveland, Ohio 44135. Refer to LEW-17065.

Mathematics and Information Sciences

Software for Obtaining Ideal SAR Chirps

A computer program introduces a predistortion into the chirp signal used to frequency-modulate a synthetic-aperture-radar (SAR) signal at the transmitter. The predistortion is intended to compensate for distortions introduced by nonideal performance of the various pieces of SAR equipment — especially the transmitter. More specifically, the predistortion is intended to make the signal in the receiver an ideal SAR signal in that it exhibits optimum correlation performance. The program is run as a calibration routine. It is used in conjunction with a closed calibration loop that includes the SAR transmitter and receiver, plus an arbitrary-waveform generator (AWG), which generates the predistorted chirp under computer control. The program causes the AWG to adjust the predistorted chirp iteratively until the chirp in the receiver differs from an optimum or reference chirp by less than a prescribed small measure of error. In a test in which a bad elliptical filter was used to simulate (with respect to distortion) the transmitting and receiving equipment of an SAR system, the program succeeded in generating a simulated receiver chirp within less than 1 dB of optimum.

This program was written by Andrew Berkun of Caltech for **NASA's Jet Propulsion Laboratory**. *Further information is contained in a TSP [see page 1].*

This software is available for commercial licensing. Please contact Don Hart of the California Institute of Technology at (818) 393-3425. Refer to NPO-20420.

BLANK PAGE

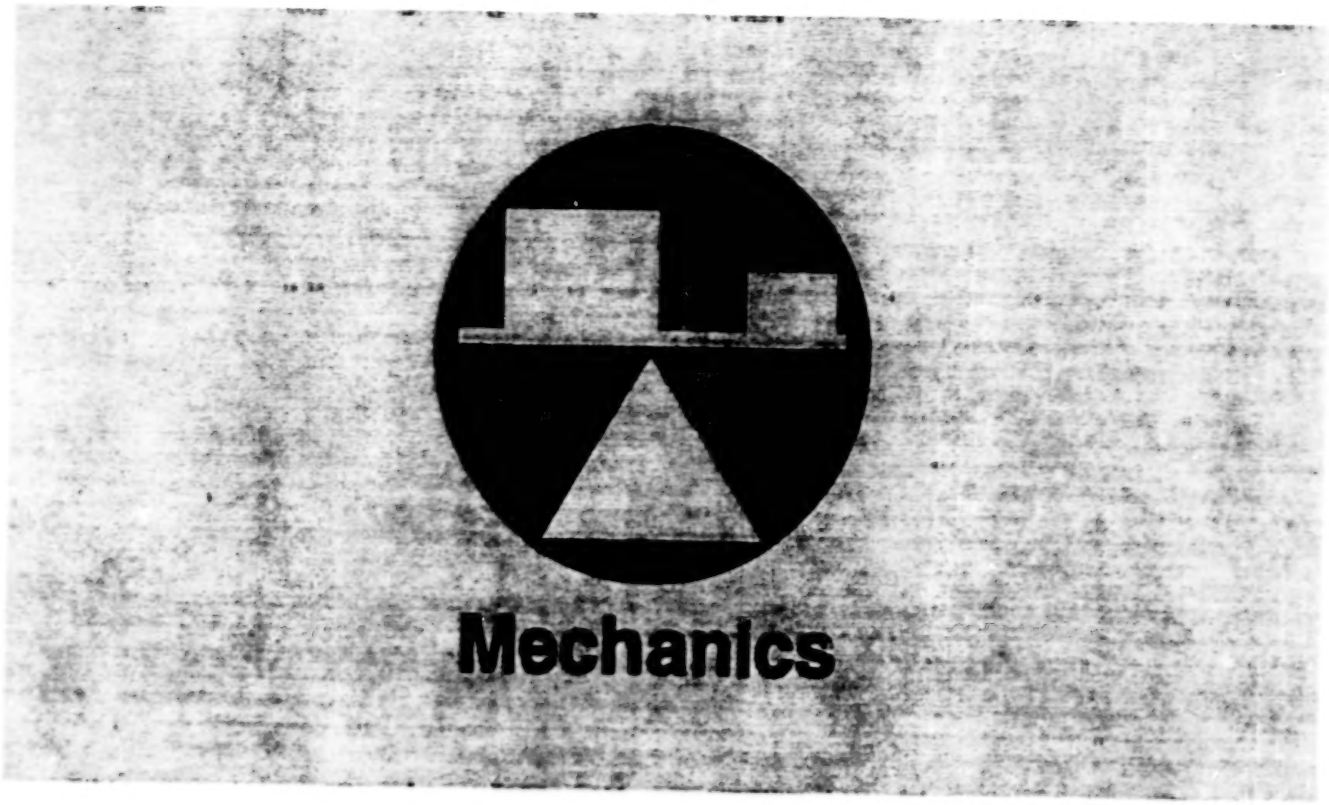

Hardware, Techniques, and Processes

33 Software Predicts Impacts of Orbital Debris on Spacecraft
34 Interlocking Wing-Leading-Edge Thermal-Protection Tiles
35 Closed/Momentary-Opening/Closed Solenoid Valve
36 Formulation and Algorithm for Multi-Flexible-Body Dynamics

BLANK PAGE

Software Predicts Impacts of Orbital Debris on Spacecraft

This program performs impact simulations faster than do conventional hydrocodes.

Lyndon B. Johnson Space Center, Houston, Texas

The EXOS computer program numerically simulates impacts of orbital debris on spacecraft. EXOS can be used to simulate meteoroid- and orbital-debris-impact damage to commercial satellites, and to simulate effects of weapons on personal and vehicular protection systems. With further development, the simulation technique employed in the EXOS package could be adapted for use in structural applications; for example, to simulate crashes in evaluating designs of vehicles.

EXOS includes a preprocessor subprogram, an analysis code, and a simple rezoner subprogram, for use in simulating large-strain thermoelastic-plastic continuum dynamics, including contact-impact effects. Commercial graphics codes are used to postprocess simulation data. EXOS implements a hybrid particle/finite-element method and is an alternative to prior Lagrangian, Eulerian, and particle-based impact codes.

In the present method, Hamilton's equations are applied to a system of translating, deforming, and thermomechanically interacting physical particles, to obtain a three-dimensional hydrodynamical model for shock-physics simulations. The method is energy-based and, hence, simple to formulate, with no need to consider continuum balance laws, interpolation functions, or weighted-residual solution techniques. Inasmuch as equations of particle kinematics, energy functions, and constraints are fully Lagrangian in form, the method makes it possible to avoid the diffusion problems typically associated with interpolation on space-fixed meshes and the stability problems observed in some moving interpolations.

Although previous methods have involved limited use of entropy states, total-entropy variables appear in this method as generalized coordinates for the particles, subject to nonholonomic thermal constraints that describe conduction of heat and dissipation of energy. Additional nonholonomic constraints on the particle coordinates and deformation gradients are introduced to represent mechanical interaction of the particles; this approach makes it possible to avoid the introduction of essentially Eulerian potential-energy functions or the remapping of data between the particles and a grid to quantify collision forces. Finally, the use of a fully Lagrangian frame of reference means that

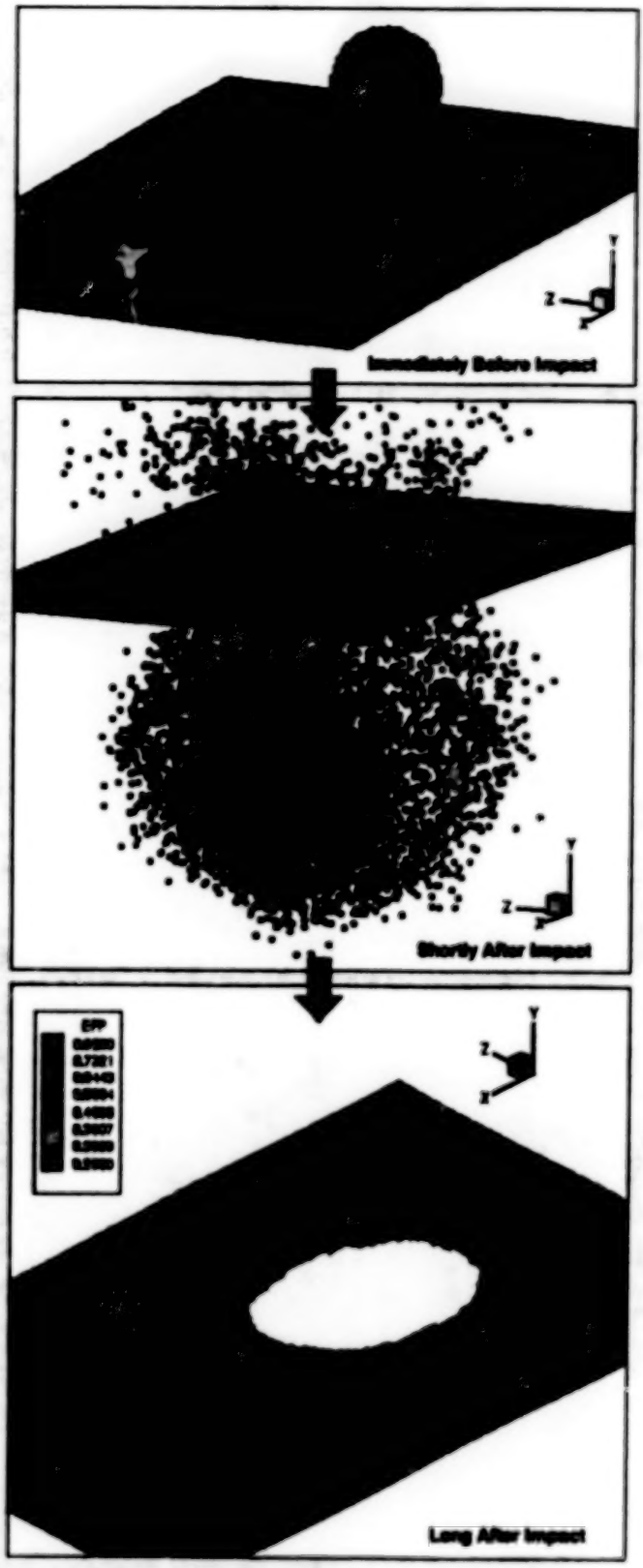

These Images Are Results of a Computational Simulation of hypervelocity impact of an aluminum sphere on an aluminum plate.

no mixing or partial pressures are needed to represent the multimaterial case.

EXOS is a three-dimensional implementation of the aforementioned particle method with an extension to include a finite-element-based description of material-strength effects, suitable for use in the simulation of hypervelocity impacts. In comparison with conventional continuum hydrocodes that have been used previously to solve orbital-debris-impact problems, EXOS is faster and more robust. Although numerous codes have been used in the past to simulate impacts of meteoroids and debris on spacecraft shields, in general they have proven very difficult to apply to three-dimensional simulations.

The figure presents selected results from an EXOS simulation of the impact of an aluminum sphere of diameter 0.953 cm on an aluminum plate of thickness 0.1143 cm at a speed of 6.56 km/s and an angle of 45°. The first image depicts the situation immediately before impact, the second image shows the situation 6.6 μs after impact, and the third image shows the resulting hole in the plate. The color contours depict accumulated plastic strain. The results of simulation have been found to be in substantial agreement with a radiograph taken in an experiment that corresponds to the simulation and that was reported in NASA Contractor Report 4707 (by A. J. Piekutowski, dated February 1996).

Johnson Space Center is working closely with the University of Texas to validate the use of EXOS in predicting the results of hypervelocity impacts on spacecraft shields. In the course of this verification process, EXOS has been modified and improved. The verification process was continuing at the time of reporting the information for this article.

Johnson Space Center is taking advantage of the stability and speed of EXOS to perform shield-impact simulations at its Hypervelocity Impact Technology Facility. Other agencies and companies involved in effects of hypervelocity impacts and protection of spacecraft could benefit from this code. With further development, its range of applications could be expanded.

This work was done by Eric P. Fahrenthold of the University of Texas at Austin for **Johnson Space Center**. *Further information is available in the article, "Hamiltonian Particle Hydrodynamics," by E. P. Fahrenthold and J. C. Koo, published in the journal Computer Methods in Applied Mechanics and Engineering, Volume 146 (1997), pp. 43-52.*

In accordance with Public Law 96-517, the contractor has elected to retain title to this invention. Inquiries concerning rights for its commercial use should be addressed to

Eric P. Fahrenthold, Professor
Dept. of Mechanical Engineering
University of Texas
Mail Code C2200
26th Street and San Jacinto
Austin, TX 78712

Refer to MSC-22979, volume and number of this NASA Tech Briefs *issue, and the page number.*

Interlocking Wing-Leading-Edge Thermal-Protection Tiles

These tiles are shaped to prevent damage at inter-tile gaps.

Ames Research Center, Moffett Field, California

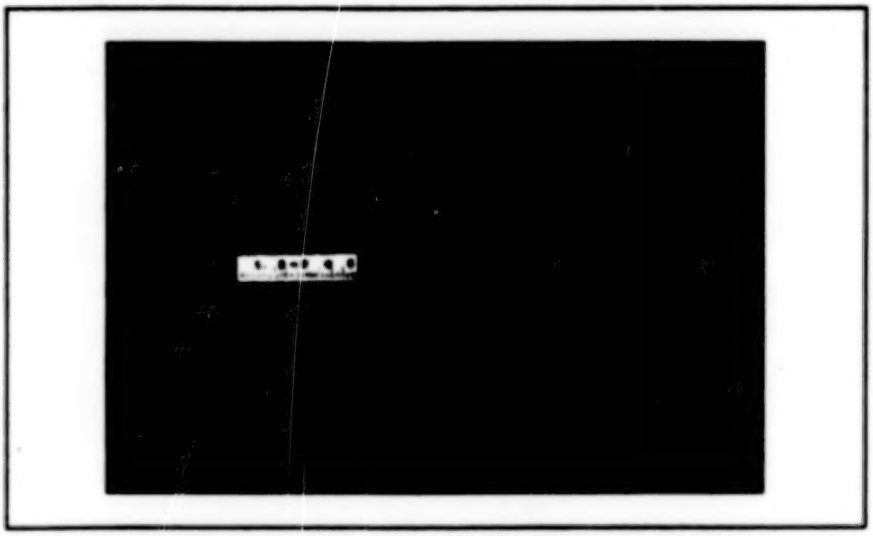

Figure 1. Damage Occurred in the Gap of a model of a straight-gap pair of tiles without filler that was subjected to a surface temperature of 2,300 °F (1,260 °C) in an arc-jet flow.

Insulating tiles with interlocking shaped gaps have been developed for use in protecting the leading edges of the wings of aerospacecraft against excessive heating during hypersonic flight (including re-entry into the atmosphere). Other thermal-protection systems have been studied for this application, including those based on active transpiration cooling and heat-sink concepts. These systems have been described extensively in literature during the past thirty years and recently have been proposed for use on two hypersonic vehicles: the National Aerospace Plane (NASP) and the Slender Hypervelocity Aerothermodynamic Research Probe (SHARP). However, because these systems are very heavy and are expensive (millions of dollars) to fabricate and to install, the probability of using these systems in the near term on the surfaces of commercially operated reusable launch vehicle is low.

Currently, the leading-edge surfaces on such vehicles as the space shuttle orbiter and X-34 reusable launch vehicle use reinforced carbon/carbon and/or ceramic tiles with a straight gap configuration. In straight-gap tile systems, it is necessary to use gap fillers to prevent hot boundary-layer gases from flowing though the gaps and creating what is known as nozzle flow. Because of the limitations of the materials available for making gap fillers, the straight gap configuration is restricted to temperatures no more than about 2,000 °F (=1,090 °C). Without a gap filler, the high-energy boundary-layer gases that are generated along a stagnation streamline (leading edge) during entry into the atmosphere would cause major damage to adjoining tiles and would cause overheating of the structure underlying the tiles. Figure 1 shows an example of damage in the gap of a model of a straight-gap pair of tiles without filler.

The interlocking-tile concept (see Figure 2) was proposed to prevent damage in the gaps between tiles. A suitable interlock

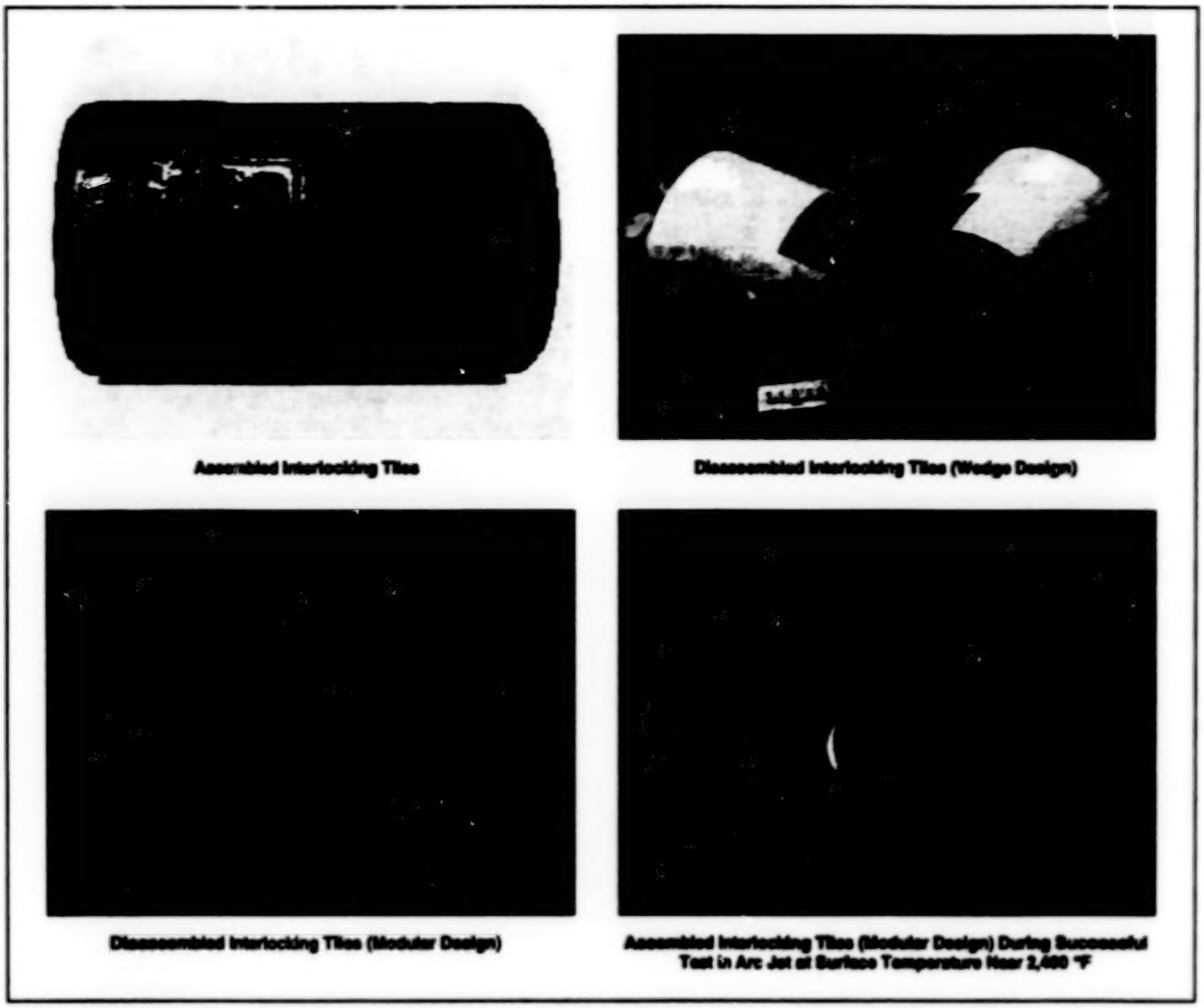
Assembled Interlocking Tiles
Disassembled Interlocking Tiles (Wedge Design)
Disassembled Interlocking Tiles (Modular Design)
Assembled Interlocking Tiles (Modular Design) During Successful Test in Arc Jet at Surface Temperature Near 2,480 °F

Figure 2. Interlocking Tiles, when properly shaped, are less vulnerable to damage in the gaps than are straight-gap tiles.

configuration divides a gap into regions of subsonic and supersonic flow regimes. The flow in the portion of the gap in the area of the stagnation streamline is subsonic. The flows in the portions of the gap in the outer portions of the tile (these portions are called bleed gaps) are in the supersonic regime of the affected leading-edge component. This concept substantially reduces the temperatures down the side wall of the gap by reducing the pressure drop through the gap below a value that can generate nozzle flow. Two patented configurations of this type, called wedge and modular, have been proposed for protecting the leading edges of wings on commercial aerospace vehicles. Tiles of these configurations have withstood arc-jet-flow tests at surface temperatures above 2,800 °F (greater than about 1,540 °C), without incurring damage in their gaps.

This work was done by David A. Stewart of **Ames Research Center**.

This invention has been patented by NASA (U.S. Patent No. 5,772,154). Inquiries concerning nonexclusive or exclusive license for its commercial development should be addressed to the Patent Counsel, Ames Research Center, (650) 604-5104. Refer to ARC-14031.

Closed/Momentary-Opening/Closed Solenoid Valve

A poppet would be toggled between two "closed" positions.

NASA's Jet Propulsion Laboratory, Pasadena, California

A proposed solenoid-actuated valve would open for a short time to pass a very small quantity of fluid. The valve could be used to meter a specified total quantity of the fluid through repeated actuations.

In the operation of a typical solenoid-actuated, momentary-opening valve of older design, the solenoid is first actuated to magnetically pull a poppet away from a valve seat to effect opening. Shortly thereafter, the current in the sole-

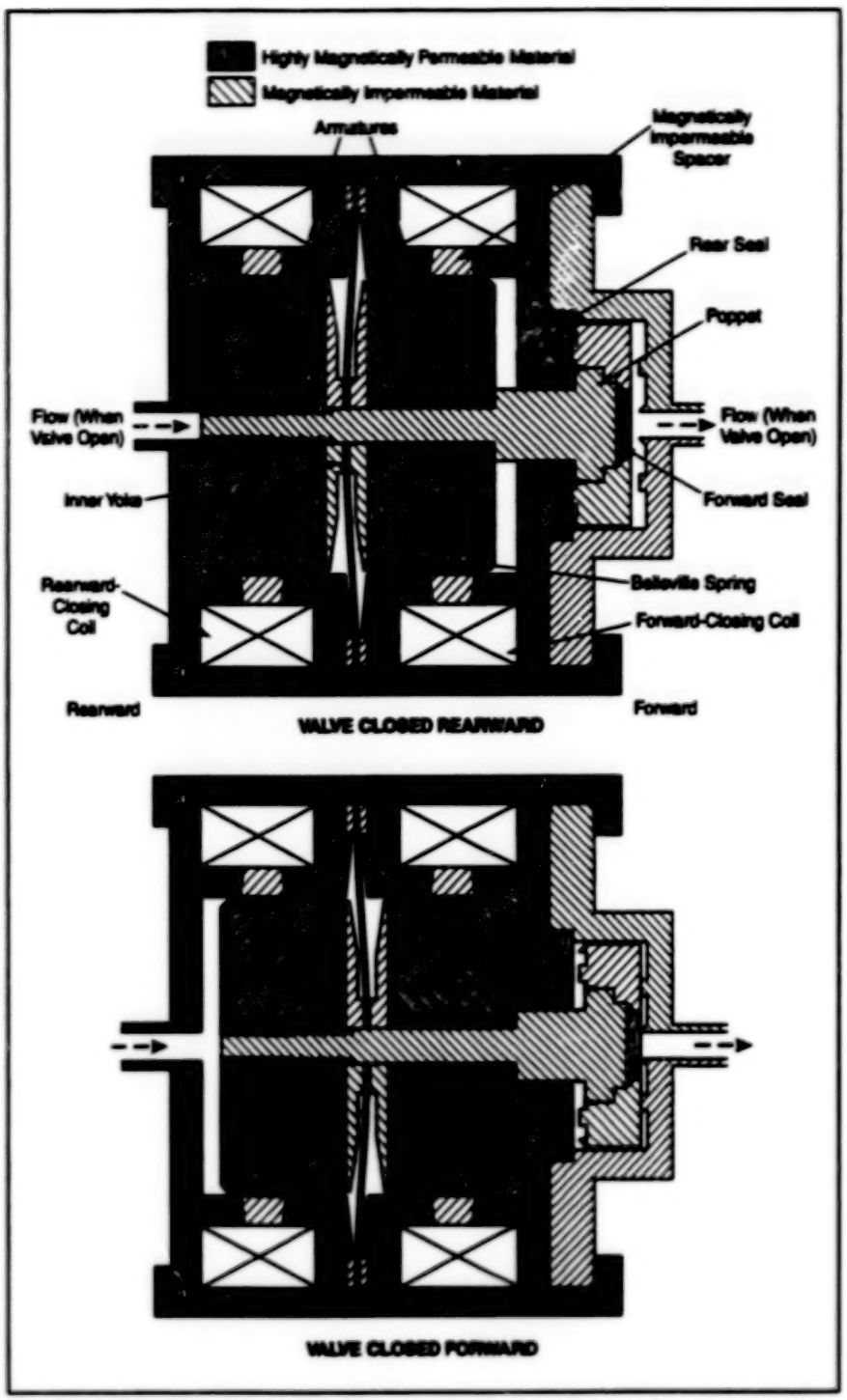

The Poppet Would Remain in either the rearward or the forward "closed" position, except for brief intervals during which one of the coils was energized to move the poppet to the other "closed" position.

noid is turned off, allowing a spring to halt the motion of the poppet away from the seat and then push the poppet back into the seat to effect closure. In the proposed valve, there would be no return stroke; instead, to effect momentary opening, the poppet would be toggled between two "closed" positions. One advantage offered by this approach would be that without a return stroke, a shorter opening time could be achieved. Another advantage would be protective redundancy; if a leak were detected with the poppet in one of the two "closed" positions, one could simply switch the valve to the other "closed" position.

In the proposed valve (see figure), a poppet would be spring-loaded and latched into either a rearward or a forward "closed" position. The spring-loading and latching action would be effected by a Belleville spring, which would be stable in either "closed" position and would snap ("oil-can") between the two stable positions when the poppet was moved through the middle position. Two armatures (magnetically permeable plungers) would be mounted on the poppet, separated by an inner yoke. There would be two solenoids; a forward-closing and a rearward-closing coil.

The armatures would be positioned, relative to the solenoids, to configure the magnetic-flux paths to obtain the desired magnetic forces. The configuration would be such that upon application of electric current to the forward- or rearward-closing coil, the resulting magnetic force would pull the poppet toward either the forward or the rearward "closed" position, respectively. When neither coil was energized, the force of the Belleville spring would hold the poppet in whichever "closed" position was reached most recently.

This work was done by George Yankura of Caltech for **NASA's Jet Propulsion Laboratory**. *Further information is contained in a TSP [see page 1].*
NPO-20596

Formulation and Algorithm for Multi-Flexible-Body Dynamics

Subroutines can be executed independently at different frequencies to optimize computer performance.

Lyndon B. Johnson Space Center, Houston, Texas

An improved formulation of the dynamics of multiple flexible bodies coupled via joints, and an algorithm that implements the formulation, have been developed at Johnson Space Center (JSC). A robot arm with multiple, somewhat flexible links is a prime example of a dynamic system to which the formulation and algorithm are intended to be applied. Other potential domains of application could include spacecraft, aircraft, industrial, automotive, and marine systems. The goal in developing the formulation and algorithm was to increase the efficiency of computational simulations of

the dynamics of all such systems.

Algorithms and computer programs that simulate dynamics ("dynamics simulators" for short) have become necessary for designing and operating increasingly sophisticated systems — especially in the case of spacecraft. As simulated systems become more sophisticated and more complex (thus increasing the amounts of computation needed to simulate their dynamics), increases in computational efficiency are needed to keep computation times as short as possible.

Prior dynamics simulators, of which there are many, can mostly be characterized as belonging to either of two general methods: the recursive Newton-Euler (NE) or the recursive projection (Lagrange-Kane) method. An attempt to base a dynamics simulator on either method results in inherent computational inefficiency for either a flexible- or a rigid-body problem for the following reasons:

- The recursive projection method also requires, among other things, the computation of a system-level mass matrix. In the case of a flexible-body problem, a system-level mass matrix is necessary for finding eigensolutions and for performing the modal truncations necessary to reduce computation time sufficiently for real-time applications. Therefore, the recursive projection method is better suited for a flexible-body problem. On the other hand, because the recursive projection method requires a system-level mass matrix even though such a matrix is not needed to solve a rigid-body problem, it is less computationally efficient when applied to such a problem.
- The recursive NE method does not require the computation of a system-level mass matrix and, because it does not, it cannot be used by itself to solve a flexible-body problem. On the other hand, because it does not require a system-level mass matrix, it is more computationally efficient for solving a rigid-body problem. In order to be able to apply the recursive NE method to a flexible-body problem, it is necessary to perform additional computations to construct the system-level mass matrix.
- Each of the recursive Newton-Euler (NE) and recursive projection (Lagrange-Kane) methods requires (1) both an inbound and an outbound recursion pass and (2) incorporation, into each dynamics simulator, of a tree-branch-indexing scheme to track the inbound and outbound recursions.

Unlike the formulations of recursive NE and recursive projection dynamics simulators, the formulation of the JSC dynamics simulator is based solely on body-to-body relations. As a consequence, there is no concept of branches in the algorithm; instead, there is only the relation of the current body to the previous body, as specified in a list of bodies. As a further consequence, only one recursion pass is necessary.

In the JSC dynamics simulator, the base body of a given system structure can be fixed or free. Each subsequent body, if any, can be attached to its parent body via joints characterized by any combination of 3 rotational or 3 translational degrees of freedom. Each body in the system can be wholly or partly rigid or flexible in any one or all of three dimensions.

The JSC dynamics simulator is designed to partition data and associated computations for multiprocess, multifrequency computation. The algorithm includes a set of subroutines that can be executed independently, at different frequencies, to optimize the computational performance in a given application. All of the subroutines work together to produce a complete dynamical solution, but computation time can be reduced, at the cost of lower fidelity, by lowering the frequencies of execution of some subroutines or not calling the subroutines at all.

In the JSC dynamics simulator, the number of operations to compute the coefficients of a mass matrix has been reduced significantly, relative to the corresponding numbers from all prior dynamics simulators; because of this and because all operations to construct a mass matrix and forcing-function terms are performed recursively, the execution time is reduced tremendously. As applied to a given flexible-body problem, the JSC dynamics simulator requires only about one-third as many computations (additions and multiplications) as do dynamics simulators based on the NE and projection methods applied to the same problem.

The JSC dynamics simulator relies on the proven symmetry of the mass matrix of a dynamic system to facilitate computation of elements in the upper left portion of a system mass matrix — elements that pertain to cross-coupling between rigid- and flexible-body dynamics and that are not easily computable in terms of the lower left portion of the mass matrix. This feature is an essential part of the mathematical justification of the single-pass recursion scheme.

The JSC dynamics-simulator formulation and algorithm have exceeded expectations at JSC, where computation times for simulations of the flexible-body dynamics of the space-shuttle remote manipulator system (RMS) have been reduced significantly below those of a dynamics simulator based on the recursive projection method. Similar reductions in computation time are anticipated for other applications.

This work was done by An Huynh of LinCom Corp. for **Johnson Space Center**. *Further information is contained in a TSP [see page 1].*
MSC-22814

BLANK PAGE

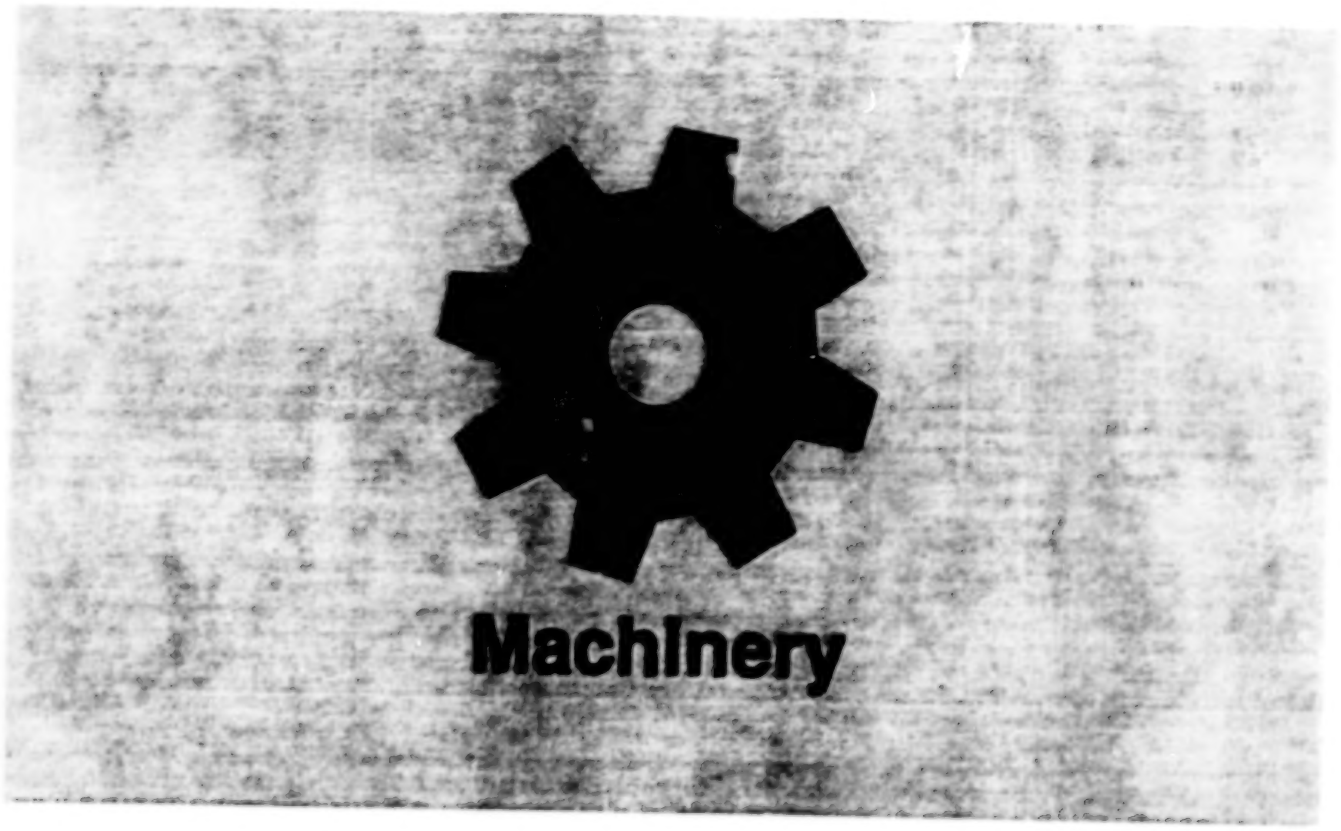

Hardware, Techniques, and Processes

41 Rolling-Piston Compressor With Flow-Through Lubrication

BLANK PAGE

Rolling-Piston Compressor With Flow-Through Lubrication

Advantages are high efficiency and insensitivity to orientation.

Lyndon B. Johnson Space Center, Houston, Texas

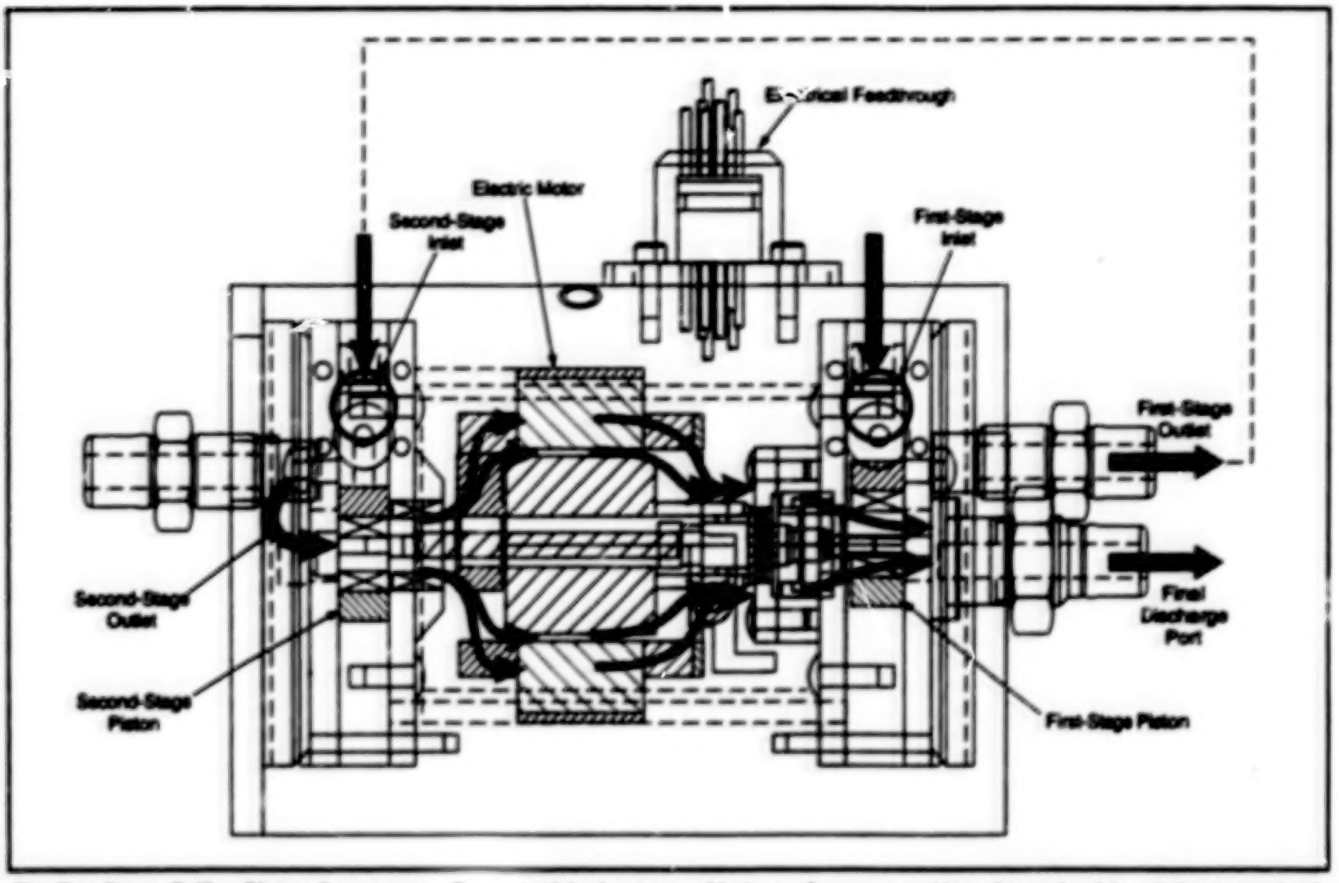

This Two-Stage, Rolling-Piston Compressor offers potential advantages of better performance and less size and weight, relative to previously developed heat-pump compressors.

The figure presents a simplified and partly schematic view of a two-stage rolling-piston compressor that is undergoing development for use as the prime mover in a vapor-compression heat pump. In comparison with equally rated compressors used heretofore in vapor-compression heat pumps, this compressor would perform better, would operate with higher efficiency, would be smaller, and would weigh less. Unlike prior compressors, this compressor could function in any orientation with respect to the gravitational field and/or acceleration, or in the absence of gravitation and acceleration.

Like most prior compressors, the present developmental compressor is designed to be part of a hermetic vapor/liquid-flow system wherein a refrigerant fluid and a lubricating oil are allowed to mix and flow together. In a typical prior compressor, a sump in the compressor housing is used to collect and hold most of the oil; this is necessary to prevent fouling of control valves and heat exchangers with excessive amounts of oil. The oil-retention function of the sump depends on the proper orientation of the sump with respect to acceleration and gravitation. In contrast, the present developmental compressor does not contain a sump; instead, as explained below, the compressor operates with flow-through lubrication, and oil is allowed to flow throughout the system. There being no sump and no need to concentrate oil at a single location in the system, the compressor and the rest of the system become insensitive to gravitation and acceleration.

The rolling-piston concept was chosen for development of this compressor for several reasons:

- Rolling pistons can readily be designed to operate at speeds greater than those of reciprocating pistons; this makes it possible to reduce sizes and weights of moving components without reducing throughput.
- The lubrication requirements of rolling-piston compressors appear to be minimal; a rolling-piston compressor can operate satisfactorily, without a sump, when lubricated by a small amount of oil (an oil mist) circulated with refrigerant.
- The requirement for low oil circulation is consistent with the need to minimize the potential for fouling of heat exchangers and control valves with oil.
- Rolling-piston compressors are quite tolerant of the entry of slugs of liquid — refrigerant or oil or both. Thus, in comparison with other compressors, rolling-piston compressors function with less dependence on precise control of liquid inventories.

A typical preliminary design calls for the developmental compressor to circulate the refrigerant fluid between an evaporator at a temperature of 240 K and pressure of about 10 psi (≈69 kPa) and a condenser (radiator) at temperature of 295 K and pressure of about 100 psi (≈690 kPa) while transferring heat from the evaporator to the condenser at rate between 300 and 500 to 500 W. The refrigerant fluid would likely be R-134a (tetrafluoroethane). The lubricant

would likely be a synthetic polyol-ester oil, the amount of oil being of the order of 10 to 20 mass percent of the refrigerant/lubricant mixture. The motor speed in typical operation would be of the order of 10,000 rpm.

Although the design calls for two stages to develop the pressure ratios needed for the required temperature lift of 55 K, both stages can be contained in a single housing, where they can be driven by one motor via one shaft. By suitable diversion of inlet and outlet flows, the two pistons can be operated in series (as two stages) to obtain a higher temperature lift at a smaller flow rate, or the two pistons can be operated in parallel (as a single stage) for a somewhat lower temperature lift at a greater flow rate. Depending on the required evaporator and condenser temperatures, a control system can select either the series or the parallel mode, whichever offers greater efficiency. The motor speed can be varied to control the capacity of the compressor in either mode.

This work was done by Daniel L. Fischbach, Russell Tetreault, Andrew C. Harvey, William Leary, Nathan Longo, and David H. Walker of Foster-Miller, Inc., for **Johnson Space Center.**
MSC-22888

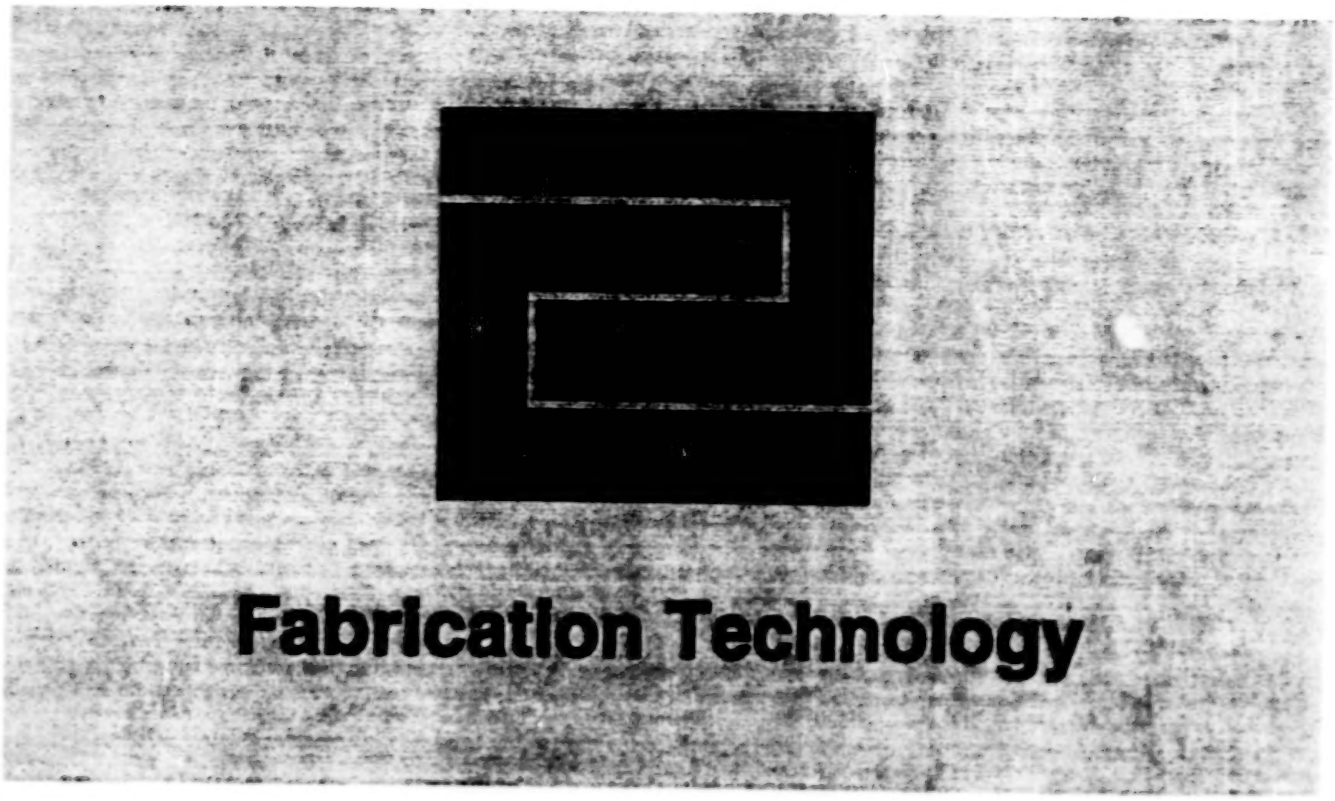

Fabrication Technology

Hardware, Techniques, and Processes

45 Glass Cure Plates for Fabricating Flat Composite Panels

45 Using Light To Fabricate Photonic Devices

BLANK PAGE

Glass Cure Plates for Fabricating Flat Composite Panels

Costs are lower than those of aluminum cure plates.

Goddard Space Flight Center, Greenbelt, Maryland

Glass plates are used as cure plates in a modified process for the fabrication of flat composite-material (matrix/fiber) panels. In the unmodified previous version of the process the cure plates were made of aluminum.

A cure plate provides a smooth, flat surface on which a polymer resin and reinforcing carbon fibers are laid up. The layup is then vacuum-bagged on the cure plate, and the polymer is cured by heating the entire assembly in an autoclave.

To be useful as cure plates, aluminum plates must be machined and polished to the required flatness and smoothness. Both the cost of material and the cost of finishing are considerable. In addition, because aluminum is soft, it is easily scratched; hence, when an aluminum cure plate is used repeatedly, costly resurfacing is necessary to maintain an acceptable cure surface.

In the modified process, an aluminum plate is used as a substrate for curing, but no attempt is made to maintain its surface finish. Instead, a glass plate is simply laid on the aluminum plate, so that the glass surface becomes the cure surface. The glass plate should be at least 1/4 in. (6.4 mm) thick, and the glass should be of a tempered or heat-resistant type.

A polymer resin and fibers are laid up on the glass plate. A vacuum bag that extends past the edges of the glass plate is placed over the layup, and is then sealed to the aluminum substrate (see figure). Then the bag is evacuated, and the resin is cured in the traditional way.

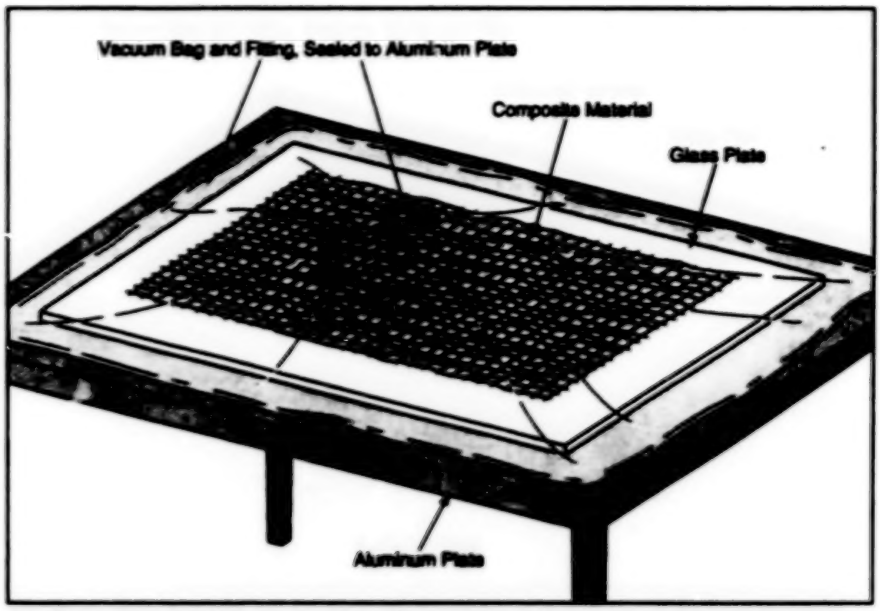

The Glass Plate provides the smooth surface needed to form a composite-material panel.

Glass cure plates offer several advantages over aluminum ones:

- Glass plates as supplied by manufacturers are adequately flat and smooth; no additional surface finishing is necessary.
- The cost of a glass plate is only about 5 percent of the cost of an aluminum plate of similar size and surface quality.
- Glass is expendable and can be replaced economically if damaged, whereas aluminum must be resurfaced.
- Being harder than aluminum, glass is less vulnerable to scratching and gouging.
- The CTE (coefficient of thermal expansion) of glass matches the CTE of composite materials more closely than does the CTE of aluminum. The cure cycle, therefore, subjects the composite to less stress and risk of damage.

This work was done by James E. Baker of **Goddard Space Flight Center.** *Further information is contained in a TSP [see page 1].*
GSC-14040

Using Light To Fabricate Photonic Devices

Pondermotive forces from patterned laser beams are used to arrange micron-sized particles.

Marshall Space Flight Center, Alabama

A developmental apparatus and process for the fabrication of photonic devices utilize intense, focused laser light projected and/or diffracted in controlled patterns. The apparatus and process can be used in a microgravitational environment to form microscopic three-dimensional device structures (e.g., filters or other periodic structures with characteristic dimensions of the order of a wavelength of light). The apparatus and process could also be used on Earth to fabricate devices with two-dimensional structures.

The apparatus is designed to generate and control the pondermotive effects of intense laser light on molecules and other small particles. These effects include radiation pressure and optical trapping forces, and are accompanied by secondary effects like dipole/dipole interactions. The process exploits these effects in order to arrange large numbers of such particles in patterns that correspond to the microscopic photonic-device structures that one seeks to fabricate.

The apparatus (see figure) includes a compact laser that generates a high-power-density beam, plus optics for either focusing the beam to a spot of adjustable size or else forming the beam into a desired pattern. The apparatus also includes a sample cell wherein the device is to be formed, external equipment (not shown in the figure) that provides controlled flows of depositional and fixative gases to the sample cell, microscopes fitted with video cameras for monitoring what happens in the sample cell, and three-dimensional (*x,y,z*) translation stages for the sample cell and for the optical components.

If, for example, a device is to be deposited on a glass plate, then the process begins with the preparation of a sample cell made from that plate (which becomes the rear plate of the cell) plus a second plate. The rear plate can be treated to enhance the adhesion of particles that are to be deposited on it. The two plates are sepa-

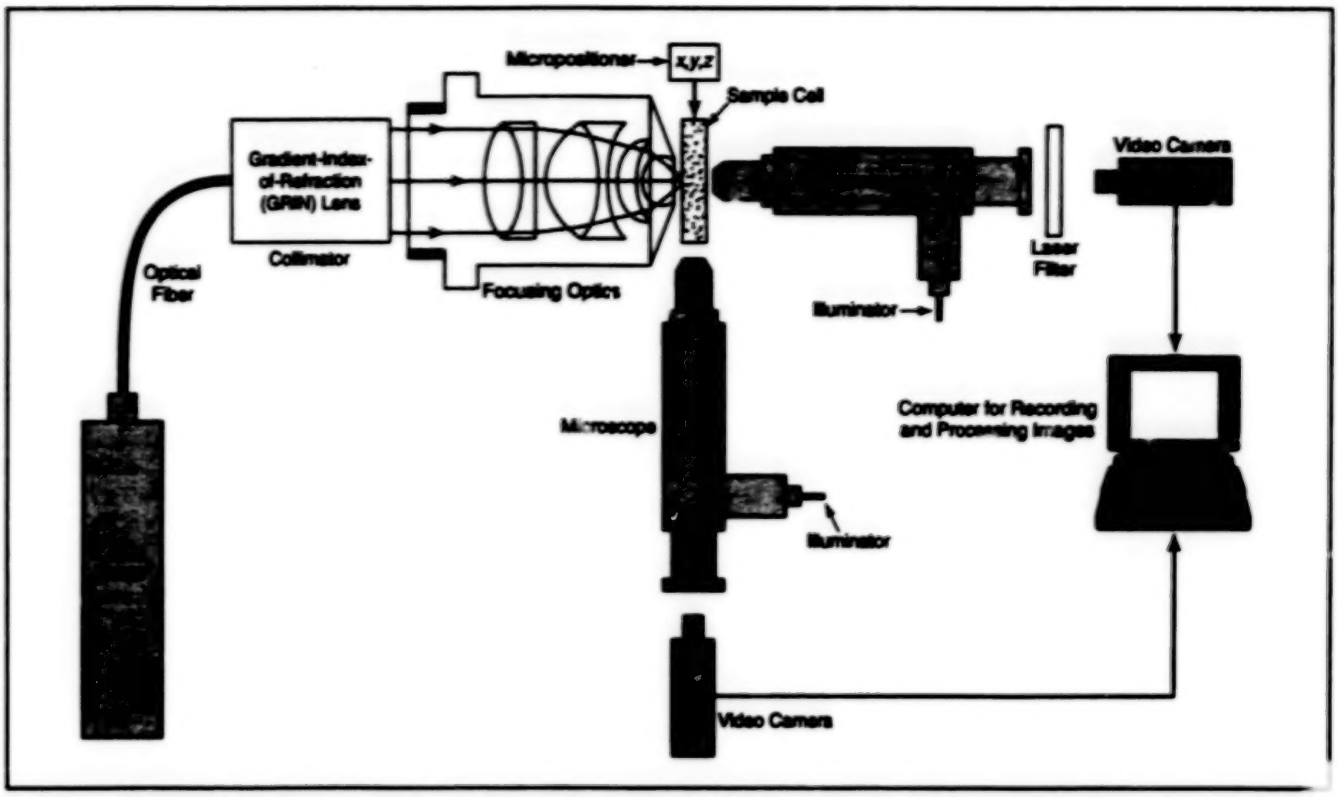

An Intense, Patterned Laser Beam is made to pass through the sample cell, wherein microscopic particles are suspended in a fluid. The pondermotive forces exerted by the laser beam on the particles arrange the particles in patterns corresponding to that of the beam.

rated by a small gap and sealed together at their edges to form the cell. A suspension of particles (typically with sizes of the order of 1 μm) is prepared and put into the cell. The laser is focused into the cell from the front side (in a gravitational field, this must be the top side). The pondermotive effects (plus gravitation, if any) push the particles onto the rear plate and arrange them in the desired pattern.

The process is not yet well defined. Preliminary experimental data have shown that crystallization in two-dimensional patterns can be achieved by controlling particle patterns as described above, but motion of the suspending fluid tends to disrupt the crystallization. Future development efforts would have to address this issue, plus the issue of fixation to make the processed material more stable.

This work was done by Laurance Malley and Sergei Krivoshlykov of ALTAIR Center, LLC, for **Marshall Space Flight Center.** *For further information, contact the company at altairctr@aol.com.*

Inquiries concerning rights for the commercial use of this invention should be addressed to the Patent Counsel, Marshall Space Flight Center [see page 1]. Refer to MFS-31360.

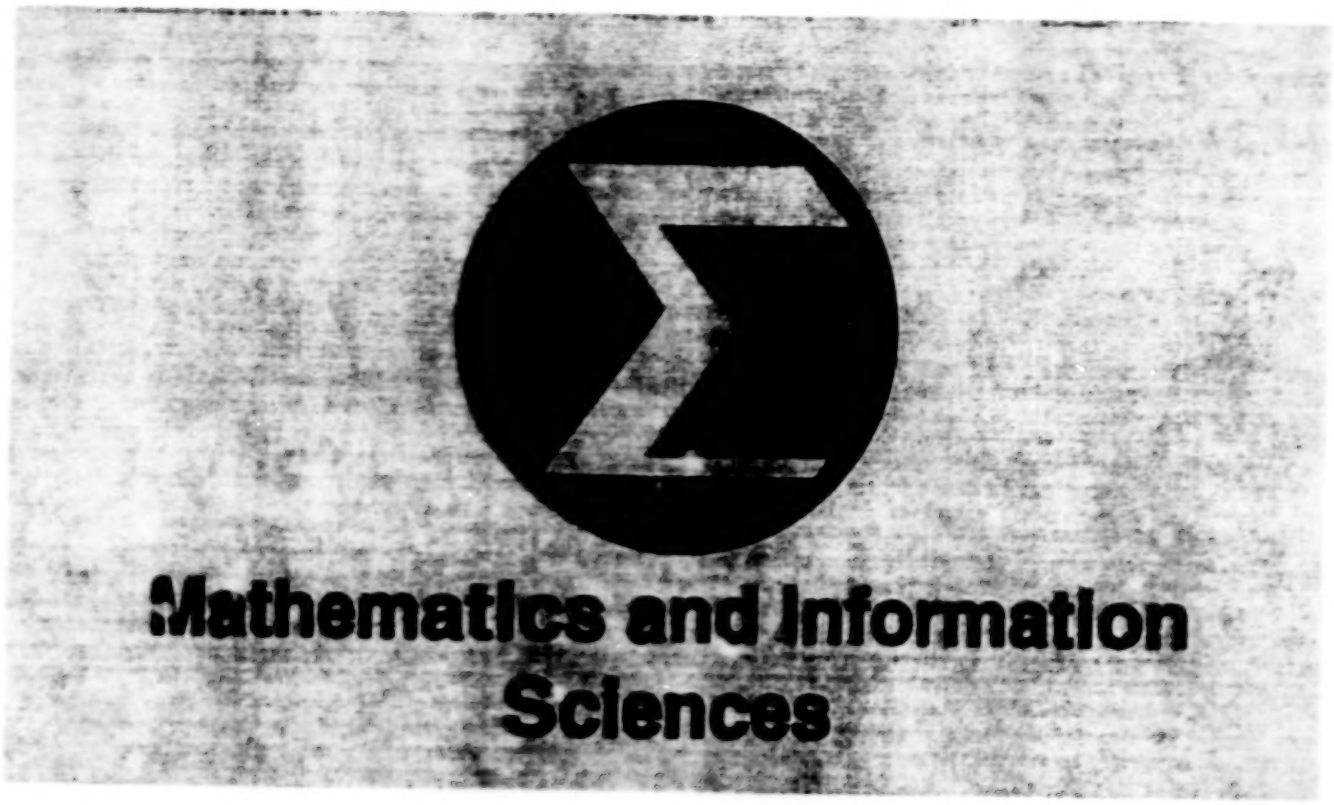

Mathematics and Information Sciences

Hardware, Techniques, and Processes

49 Analyzing Time Series Using EMD and Hilbert Spectra

50 MDICE: Software System for Multidisciplinary Computing

52 Software Assists in the Development of Optimization Models

53 Electronic Storage and Retrieval of Engineering Documents

Books and Reports

53 Interface Program for Generation of Computational Grids

BLANK PAGE

Analyzing Time Series Using EMD and Hilbert Spectra

Complicated sets of data can be decomposed into finite collections of intrinsic mode functions.

Goddard Space Flight Center, Greenbelt, Maryland

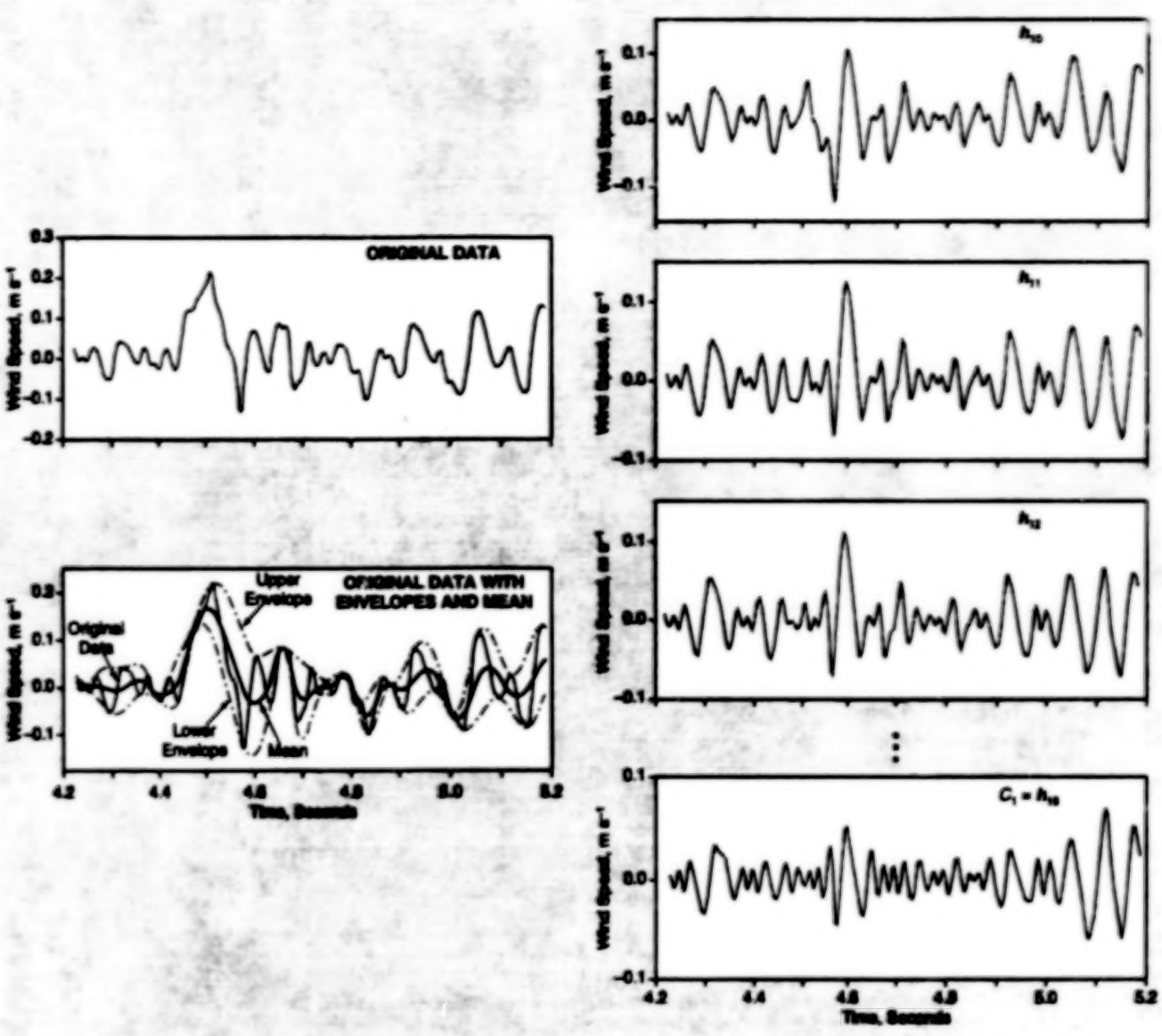

The Original Data Are Sifted in the multistep process described in the text to obtain the first IMF component.

A recently developed theoretical and computational method is especially well suited for analyzing time-series data that represent nonstationary and nonlinear processes. The method stands in contrast to classical methods, including Fourier analysis, that are generally applicable only to periodic or stationary data that represent linear processes. The present method is based principally on the concept of empirical mode decomposition (EMD), according to which any complicated set of data can be decomposed into a finite (and often small) number of functions, called "intrinsic mode functions" (IMFs), that admit well-behaved Hilbert transforms.

This decomposition method is adaptive and, therefore, highly efficient. The main innovations embodied in this method are (1) the introduction of the IMFs, which are based on local properties of the signal to be analyzed and which give meaning to the concept of instantaneous frequency; and (2) the introduction of instantaneous frequencies for complicated sets of data, which frequencies eliminate a need for spurious harmonics to represent nonlinear and nonstationary processes.

Without going into detail that would exceed the scope of this article, an IMF can be loosely defined as an oscillation mode that is embedded in the data to be analyzed and that is associated with a local time scale of the data. An IMF need not be a narrow-band signal; it can be amplitude- and/or frequency-modulated and can even be nonstationary. The formal criteria for identifying an IMF are that (1) in the whole set of data, the numbers of extrema and zero crossings must be equal or differ by 1 at most, and (2) at any point, the mean value of the envelope defined by the local maxima and the envelope defined by the local minima must be zero.

The decomposition for a given set of data is based on direct extraction of the energies associated with various time scales and can be viewed as an expan-

sion of the data in terms of the corresponding IMFs, which are derived from the data. The expansion can be linear or nonlinear, as dictated by the data, and it is complete and almost orthogonal. Most important, because the IMFs are derived from the data, the expansion is adaptive.

The locality and adaptivity are necessary for expanding nonlinear and nonstationary time series. The local energies and the instantaneous frequencies derived from the IMFs through Hilbert transforms can be used to construct a full energy-frequency-time distribution of the data. Such a distribution is denoted a Hilbert spectrum.

The EMD is based on three assumptions: (1) the signal has at least two extrema — at least one maximum and at least one minimum, (2) the characteristic time scale is defined by the time between the extrema, and (3) if the data are devoid of extrema but contain inflection points, then the data can be differentiated once or more times to reveal extrema. Final results can be obtained by integration(s) of the components.

The essence of the EMD is to identify the intrinsic oscillatory modes by their characteristic time scales, then decompose the data accordingly. The time scales are identified as the intervals between the successive alternations of local maxima and minima and by the intervals between successive zero crossings. The interlaced local extrema and zero crossings contribute to the complicated set of data to be analyzed: one undulation rides on another, and they, in turn, ride on still other undulations, and so on. Each of these undulations defines a characteristic scale of the data; it is intrinsic to the process.

The IMFs are extracted from the data in a sifting process (see figure). By virtue of the definition of "IMF", the decomposition can be effected simply by use of the envelopes defined by the local maxima and minima separately. Once the extrema are identified, all the local maxima and minima, respectively, are connected by a cubic spline line as the upper and lower envelope, respectively. The upper and lower envelopes should cover all the data between them. Their mean is designated as m_{10}. The difference between the data and m_{10} is denoted the first component, given by $h_{10} = X(t) - m_{10}$, where $X(t)$ is the datum at time t.

Ideally, h_{10} should be an IMF. In reality, overshoots and undershoots are common; they can generate new extrema and shift or exaggerate previously discovered extrema. There can remain negative local maxima and positive local minima. Thus, it becomes necessary to repeat the sifting, using h_{10} as the data: $h_{11} = h_{10} - m_{11}$, where m_{11} is the local mean of the upper and lower envelope of h_{10}. In general, it may be necessary to perform the sifting k times to arrive at the first IMF component, $c_1 = h_{1k} = h_{1(k-1)} - m_{1k}$. In the example of the figure, it is necessary to repeat the sifting up to $k = 9$ to obtain the first IMF component; that is, $c_1 = h_{18}$.

The first IMF component should be the one associated with the shortest time scale in the data. The second IMF component (c_2) associated with a longer time scale, is obtained by sifting the first residue signal $r_1 = X(t) - c_1$. In general, the nth IMF component (c_n for $n>1$), associated with a time scale longer than that of the $(n-1)$st component, is obtained by sifting $r_n = r_{n-1} - c_n$. The sifting can be stopped when either of the following criteria is satisfied: (1) c_n or r_n becomes smaller than a predetermined minimum value of substantial consequence or (2) r_n becomes a monotonic function from which no more IMF can be extracted. The sift process can be used as a time-domain filter.

This work was done by Norden E. Huang and Steven Long of **Goddard Space Flight Center**. *Further information is contained in a TSP [see page 1].*

This invention is owned by NASA, and a patent application has been filed. Inquiries concerning nonexclusive or exclusive license for its commercial development should be addressed to the Patent Counsel, Goddard Space Flight Center [see page 1]. Refer to GSC-13817.

MDICE: Software System for Multidisciplinary Computing

Programs for different disciplines can readily be incorporated as needed.

John H. Glenn Research Center, Cleveland, Ohio

The Multi-Disciplinary Computing Environment (MDICE) is a software system for multidisciplinary analysis of complex engineering equipment, processes, and systems. Currently MDICE supports a variety of disciplines, including parametric computer aided design (CAD), grid generation, computational fluid dynamics (CFD), computational structural dynamics (CSD), active controls, and visualization/animation.

MDICE has been developed by CFD Research Corporation with funding from NASA Glenn Research Center and AFRL Air Vehicles Directorate at WPAFB.

While the growing need for multicomponent and multidisciplinary engineering analysis has been understood for years, lack of integration among computer programs that serve different disciplines has posed a major obstacle to such analysis. The existence of many different formats for the various data files contributes to the general difficulty. The development of MDICE has addressed those issues.

MDICE is an extensible program suitable for integration of analysis programs from several engineering disciplines. MDICE was developed by extending a prior software system, called "Visual Computing Environment" (VCE), that had been developed to enable coupling among various flow-analysis codes. VCE has been used with success in analyzing aircraft-engine components. The MDICE system is currently being applied to a large variety of multidisciplinary analysis problems for aerospace applications. Other application areas, such as automotive, electronics, manufacturing and MEMs design, are under development.

The MDICE approach is to provide a computing environment in which many computer programs operate concurrently and cooperatively to solve a multidisciplinary problem. Execution of each computer program is controlled by an engineer via a graphical user interface generated by MDICE (see figure).Once running, these programs communicate with each other and with MDICE via a set of standard function calls. Like the execution of each program, the management of the communications among the application programs is fully controlled by the user. MDICE takes care of all data transformations necessary for data exchange between dissimilar applications and disciplines.

Integration of a particular application program into the environment is accomplished by making the application MDICE-compliant rather than writing the code to communicate with a small set of other, predetermined programs. An MDICE-compliant application program can run under the control of MDICE and communicate with any other MDICE-compliant application program.

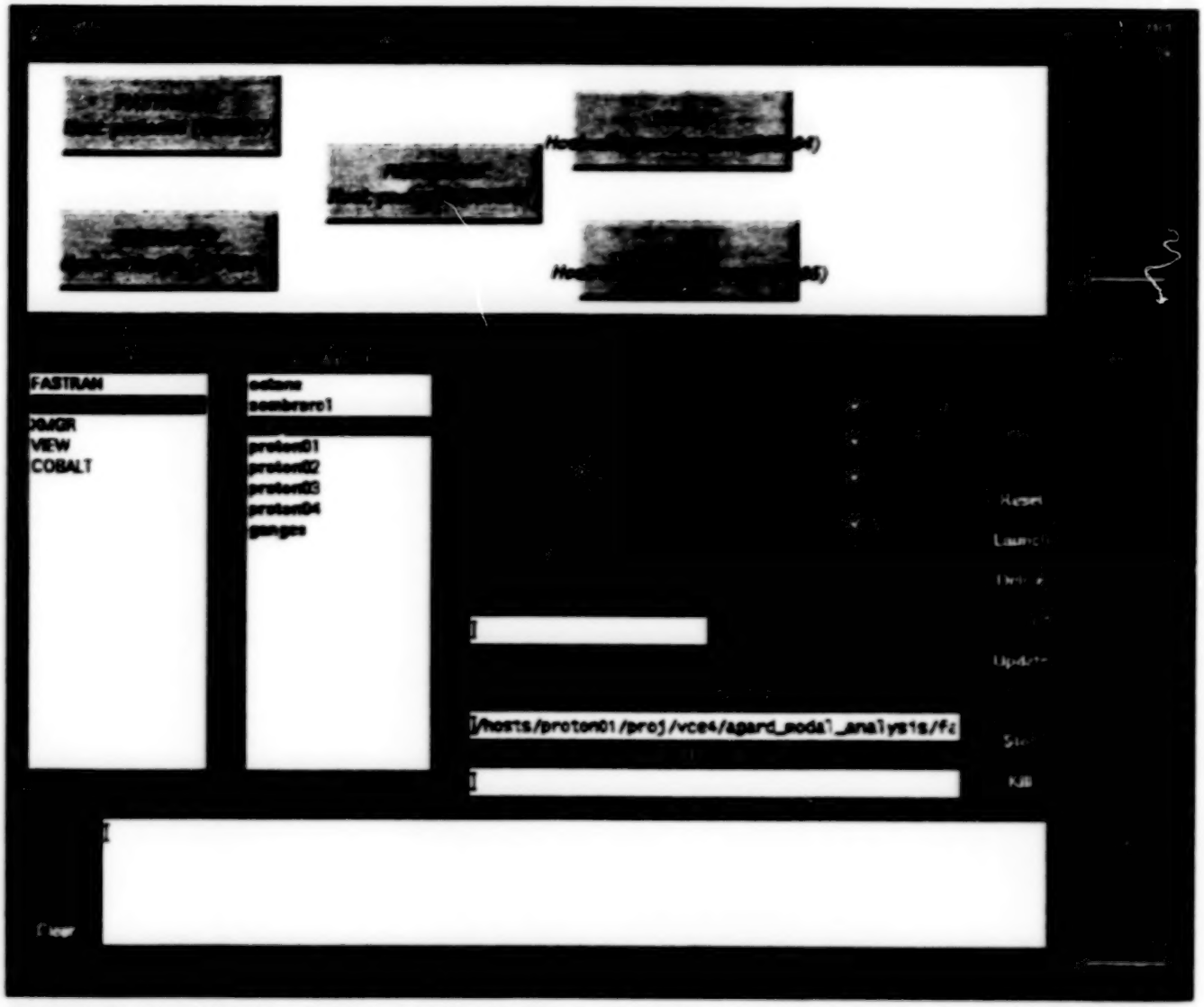

The Application Control Panel is a graphical user interface for setting up and controlling a computational simulation. Through this interactive display, a user can select an application program, select the computer on which the application program is to be run, specify a directory in which the program is to be run, and specify any command-line arguments that might be required by the program.

The use of MDICE makes it possible to avoid the need for a giant, monolithic code that one might otherwise attempt to develop to provide all the services needed in a given situation. Such large programs are difficult to develop and maintain and, by their very nature, tend not to be up to date. The MDICE approach both accommodates and relies upon the reuse of previously developed codes that have been validated and have a high level of end-user familiarity.

The MDICE environment enables flexibility in that one can readily exchange one application program for another; thus, each engineer can select and apply the software best suited to the task at hand. Efficiency is achieved by use of parallel, distributed computing architectures utilizing heterogeneous software and hardware. Extensibility is achieved by providing for the addition of new application programs without modifying or deleting application programs that have already been integrated into the environment.

A large number of engineering analysis programs from a variety of disciplines and sources have been integrated with MDICE. Examples for CAD are CFD-GEOM (CFDRC), Unigraphics (Unigraphics Solutions), and Pro/ENGINEER (Parametric Technology Corporation). CFD applications include CFD-ACE, CFD-ACE+, CFD-FASTRAN (all CFDRC), NPARC, ADPAC, CORSAIR (NASA Glenn), Cobalt, ENS3D-AE (AFRL), CGNSlv (Northrop Grumman), Splitflow (Lockheed Martin), and others. Structural analysis codes include FEMSTRESS (CFDRC), NASTRAN (MacNeal Schwendler Corp.), and ANSYS (Ansys Inc.).

Typical applications include multifidelity, multidimensionality, and multicomponent CFD analysis, fluid-structure interaction, parametric geometry and analysis, active controls, and in general any application involving moving and deforming computational grids. Planned applications include optimization, aero-servo-elasticity, and aero-thermal-elasticity.

This work was done by Charles Lawrence of **Glenn Research Center**; *Vincent J. Harrand, Gerry Kingsley, and John M. Siegel of CFD Research Corp.; and Joel J. Luker of the Air Force Research Laboratory. For further information, visit CFDRC's MDICE website at www.cfdrc.com or see TSP's [page 1].*
LEW-16830

Software Assists in the Development of Optimization Models

This program automates much of the model-development process.

John F. Kennedy Space Center, Florida

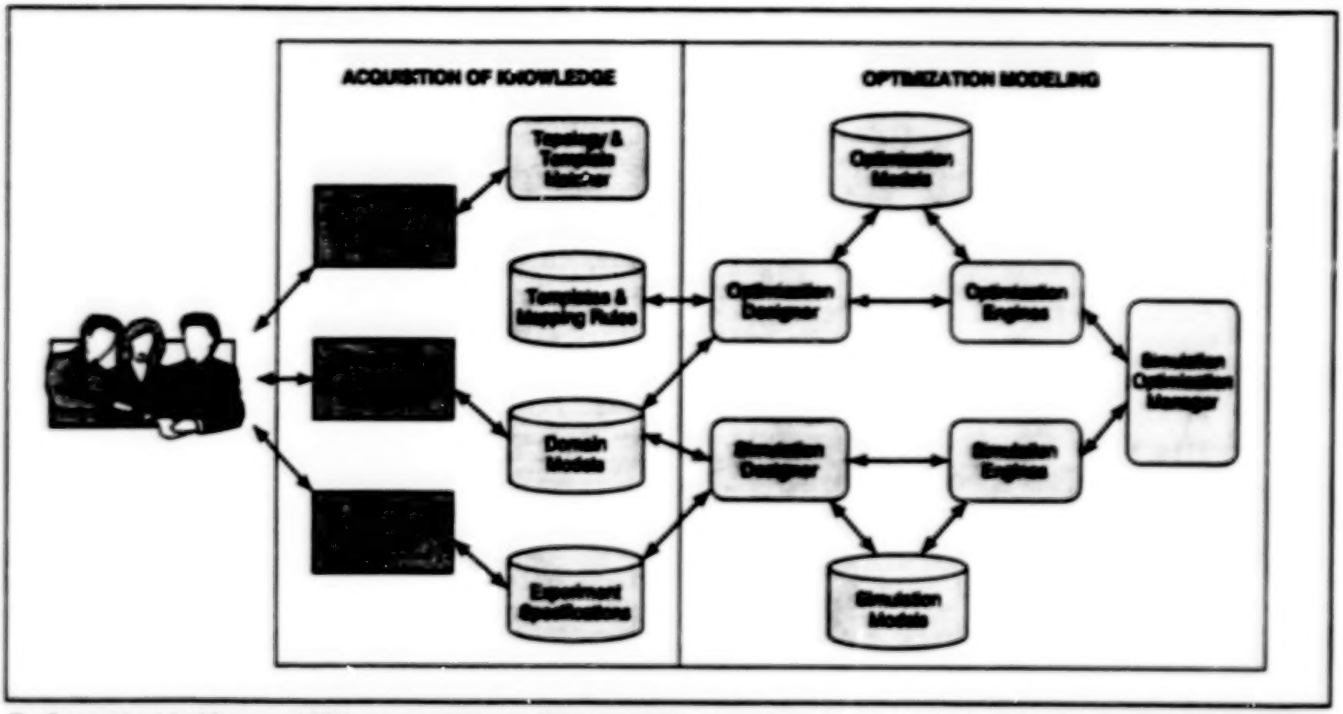

The Conceptual Architecture of OMA accommodates two distinct processes — acquisition of knowledge and optimization modeling. The architecture is modular, so that OMA can evolve and be integrated with other decision-support software tools.

Optimization Modeling Assistant (OMA) is an expert-system computer program that assists its users in the development of mathematical and algorithmic models for optimization. As used here, "optimization" refers to a suite of powerful decision-support techniques that enable the modeling of any decision-making environment in terms of the objectives, the decisions that potentially influence the objectives, and a set of constraints that bind the decisions. Optimization analysis helps decision makers in identifying decisions that optimize their objectives. Domains in which optimization modeling are applied include real-time scheduling, logistics, planning, and financial management.

Unfortunately, difficulties inherent in the construction of optimization models have prevented the realization of the full potential of optimization modeling in these and other domains. These difficulties include the following:

- Often, optimization models for a given domain address aspects of the domain that are invisible to casual observers.
- Optimization analysis is expensive because it demands highly specialized skills. A major hurdle is that domain experts are typically not expert in the techniques of optimization, and vice versa.
- Because of a lack of a comprehensive decision-support software environment, optimization-based decision-support systems typically depend on building custom solutions for different domain situations. It is often necessary to redesign such a system as the environment evolves or the requirements change.

OMA (see figure) helps to overcome the difficulties by utilizing knowledge-based-systems techniques to automate much of the model-design process. Though OMA can be used by itself, it is designed to be integrated into a more comprehensive decision-support software environment. OMA assists users in developing structured optimization models from possibly unstructured domain descriptions. The intended users of OMA include both domain experts and optimization experts who lack expertise in each others' specialties.

OMA reuses domain models to automatically generate optimization models. Domain models can be process models or ontology models. In a given application, OMA guides its user(s) through a step-by-step process, according to a structured methodology, to generate relevant and solvable optimization models from structured domain models. OMA extracts, from both the user(s) and the domain models, the information (e.g., goals and parameters) necessary for generating optimization models. OMA then automatically generates and validates the optimization models for the application. The results of the validation subprocess can be used to identify information missing from the optimization models, to identify unsatisfiable constraints, and to identify circular definitions.

The main benefits of using OMA include the following:

- Improved automated support for capturing domain-expert descriptions of systems, situations, and problems;
- Increased productivity in the selection of optimization techniques and in the design and execution of optimization models;
- Enhanced communication between domain experts and optimization analysts; and
- Reduced dependence on optimiza-

tion experts to design and use optimization models for decision-support activities.

This work was done by Peraiath C. Benjamin, Satheesh Ramachandran, and Madhav Erraguntla of Knowledge Based Systems, Inc., for **Kennedy Space Center.** *Further information is contained in a TSP [see page 1].*

In accordance with Public Law 96-517, the contractor has elected to retain title to this invention. Inquiries concerning rights for its commercial use should be addressed to

Peraiath Benjamin
Knowledge Based Systems, Inc.
1408 University Drive East
College Station, TX 77840

Refer to KSC-12135, volume and number of this NASA Tech Briefs issue, and the page number.

Electronic Storage and Retrieval of Engineering Documents

Drawings can be retrieved from a remote central site, manipulated, and printed locally.

John F. Kennedy Space Center, Florida

The KSC Electronic Documentation System (KEDS) is a computer-intranet system at Kennedy Space Center (KSC) for the storage and retrieval of engineering drawings and other engineering documents that have been officially released. Prior to the development of the KEDS, microfilm copies of engineering documents were stored in an archive at the Engineering Document Center (EDC) in the KSC headquarters building; engineers and drafters had to travel from remote sites to the EDC to view microfilm images of drawings, and the cost of fulfilling requests for documents (including printing paper copies) was considerable.

The KEDS makes it possible for customers at remote locations equipped with personal computers running any Windows operating system to retrieve the documents via the World Wide Web (WWW), view the documents, and generate paper copies on their own computer printers. Microfilm copies of documents are mounted on Hollerith aperture cards that are punched with data that identify the documents. The aperture cards are then scanned to digitize the images and the resulting image data are stored on a scan-server computer. Once a document has thus been scanned into the KEDS, there is no further need to handle either the original paper copy or a microfilm copy other than to place it in the archive. Thereafter, requests for the document copies can be fulfilled from the scanned, digitized version of the document.

The KEDS document data are eventually transferred from the scan-server to a file-server computer, where they are stored in a read-only format. The file server is a DEC VAX computer located within KSC's internet "firewall," which allows access by KSC personnel and other authorized customers only. The KEDS utilizes the standard Transmission Control Protocol/Internet Protocol (TCP/IP) for efficient transfer of electronic requests from, and images to, customers' personal computers. An application program for viewing KEDS scanned images was developed by, among other things, incorporating a commercial viewer program, with suitable regard for licensing requirements. The KEDS WWW home page provides a fully automated software-download feature, eliminating the need for costly technical-support visits to customer sites.

A customer can gain access to the KEDS through any standard WWW browser program. Once the KEDS home page is displayed on a customer's computer screen, the customer can obtain instructions for downloading and configuring the KEDS viewer software. The KEDS server gathers identifying information entered by the customer via a download-request page; this information is stored in a data base. Once the customer has downloaded and configured the viewer software, the customer types in a number that identifies a package of engineering documents; in response, a list of available drawings and/or other documents is displayed. When the user selects the drawing sheet or other document from the list, the viewer software is invoked automatically.

The user software provides options for panning, zooming, rotating, printing, and cut-and-paste operations on a displayed KEDS image. By use of the cut-and-paste option, the image can be inserted easily into documents produced by other Windows-based application programs, including spreadsheet and word-processing programs. The standard Windows printer-interface forms can be used for local and/or networked printing of any view of a drawing.

This work was done by Donna L. Pancho, Richard Hall, and Dale L. Hirchert formerly of EG&G Florida, Inc., for **Kennedy Space Center.** *Further information is contained in a TSP [see page 1].*

Inquiries concerning rights for the commercial use of this invention should be addressed to the Technology Programs and Commercialization Office, Kennedy Space Center, (407) 867-6373. Refer to KSC-11958.

Books and Reports

Interface Program for Generation of Computational Grids

Computer Aided Grid Interface (CAGI) is a computer program that serves as an interface between computer-aided design/computer-aided manufacturing (CAD/CAM) programs and computational fluid dynamics (CFD) programs. CAGI reads Initial Graphics Exchange Specification (IGES) files from CAD/CAM programs and converts from CAD/CAM geometries to nonuniform rational B-splice (NURBS) surfaces to be manipulated or written out in forms appropriate for generation of grids for CFD.

This work was done by Tzuyi Robert Yu and Bahrat Soni of Mississippi State University for **Marshall Space Flight Center.** *For further information, contact Larry Gagliano, MSFC Software Release Authority, at (256) 544-7175 or larry.gagliano@msfc.nasa.gov.*

MFS-31302

END

12-4-01